



Original Paper

A tectono-thermal perspective on the petroleum generation, accumulation and preservation in the southern Ordos Basin, North China



Peng Yang^{a,*}, Zhan-Li Ren^{a,**}, Jin-Hua Fu^b, Hong-Ping Bao^b, Hui Xiao^c, Zheng Shi^d,
Kun Wang^a, Yuan-Yuan Zhang^b, Wen-Hui Liu^{a,d}, Wen-Hou Li^a

^a State Key Laboratory of Continental Dynamics, Department of Geology, Northwest University, Xi'an, 710069, Shaanxi, China

^b National Engineering Laboratory for Exploration and Development of Low-Permeability Oil and Gas Fields, Exploration and Development Research Institute of PetroChina Changqing Oilfield Company, Xi'an, 710018, Shaanxi, China

^c Shaanxi Key Lab of Petroleum Accumulation Geology, School of Earth Science and Engineering, Xi'an Shiyou University, Xi'an, 710065, Shaanxi, China

^d Wuxi Research Institute of Petroleum Geology, Petroleum Exploration and Production Research Institute, SINOPEC, Wuxi, 214126, Jiangsu, China

ARTICLE INFO

Article history:

Received 21 February 2023

Received in revised form

18 May 2023

Accepted 5 December 2023

Available online 22 December 2023

Edited by Jie Hao and Meng-Jiao Zhou

Keywords:

Fission-track dating

Vitrinite reflectance

Geothermal field

Tectono-thermal evolution

Petroleum geology

Ordos Basin

ABSTRACT

The southern Ordos Basin has excellent petroleum exploration prospects. However, the tectono-thermal history and the controls on petroleum generation, accumulation and preservation conditions in southern basin are unclear. In this study, we analyzed the present geothermal field, paleo-geothermal gradient, maturity of the hydrocarbon source rocks, uplift and cooling process and tectono-thermal evolution history. In the study area, for the Ordovician, Permian and the Triassic strata, the present temperature is low (30–70 °C) in the southeastern area but high (80–140 °C) in the northwestern area. The paleo-geothermal gradient varied from 24 °C/km to 30 °C/km with a heat flow of 58–69 mW/m² (i.e., a medium-temperature basin). The paleo-temperatures are higher than the present temperatures and the maximum paleo-temperatures controlled the thermal maturity of the source rocks. The vitrinite reflectance (R_o) values of the Triassic strata are >0.7% and the thermal maturity reached the middle-mature oil generation stage. The R_o values of the Permian-Ordovician strata are >1.8% and the thermal maturity reached the over-mature gas generation stage. The southern Ordos Basin has experienced the multiple tectonic events at the Late Ordovician Caledonian (452 Ma), Late Triassic (215 Ma), Late Jurassic (165–160 Ma), End-Early Cretaceous (110–100 Ma) and Cenozoic (since 40 Ma). A large-scale tectono-thermal event occurred at the End-Early Cretaceous (110–100 Ma), which was controlled by lithospheric extension, destruction and thinning. This event led to the highest paleo-temperatures and thermal maturities and coeval with the peak period of petroleum generation and accumulation. The southern Ordos Basin has undergone rapid and large-scale uplift since the Late Cretaceous due to expansion of the northeastern margin of the Tibetan Plateau, uplift of the Qinling orogenic belt and thrust faulting in the Liupanshan tectonic belt. The southern Ordos Basin experienced tectonic overprinting that was strong in the south and weak in the north. The strongest overprinting occurred in the southwestern part of the basin. The large-scale uplift, denudation and faulting led to oil and gas loss from reservoirs. The petroleum generation, accumulation and preservation in the southern Ordos Basin were affected by deep lithospheric structures and the tectono-thermal evolution. This work provides a novel tectono-thermal perspective on the petroleum generation, accumulation and preservation condition of the southern Ordos Basin.

© 2023 The Authors. Publishing services by Elsevier B.V. on behalf of KeAi Communications Co. Ltd. This is an open access article under the CC BY-NC-ND license (<http://creativecommons.org/licenses/by-nc-nd/4.0/>).

* Corresponding author.

** Corresponding author.

E-mail addresses: p.yang@nwu.edu.cn (P. Yang), renzhanl@nwu.edu.cn (Z.-L. Ren).

<https://doi.org/10.1016/j.petsci.2023.12.006>

1995-8226/© 2023 The Authors. Publishing services by Elsevier B.V. on behalf of KeAi Communications Co. Ltd. This is an open access article under the CC BY-NC-ND license (<http://creativecommons.org/licenses/by-nc-nd/4.0/>).

1. Introduction

The Ordos Basin is one of the largest sedimentary basins in northwestern China, with a total area of 3.7×10^5 km², and is

located along the northeastern margin of the circum-Tibetan Plateau basins and orogenic system (Fig. 1(a)). The Ordos Basin contains abundant oil and natural gas resources and is a sedimentary basin with one of the high oil and gas production rates in China (Fig. 1(b), Ren et al., 2007, 2014a, 2017; Du et al., 2019; Fu et al., 2019; Yang et al., 2021a, 2021c). Large-scale oil and gas fields have been discovered in the Mesozoic and Upper Paleozoic strata of the southern Ordos Basin (Ren et al., 2014b; Wang et al., 2014). In addition, the petroleum also occurs in the Lower Paleozoic Ordovician and Proterozoic-Archean strata (Fig. 1(c)). Due to the development of deep and ultra-deep oil and gas exploration, the oil and gas potential of Lower Paleozoic-Precambrian strata has been investigated (Ma et al., 2010; Sun et al., 2013; Zhao et al., 2014; Jia and Pang, 2015; Ren et al., 2020a, 2020c; Cao et al., 2022). Deep oil and gas exploration in Cambrian-Ordovician and Precambrian strata in the Tarim and Sichuan basins has been highly successful (Ma et al., 2010; Qi, 2016; Dai et al., 2018; Tian et al., 2020; Yang et al., 2020, 2021b). However, in the Lower Paleozoic strata of the Ordos Basin, apart from the discovery of the Jingbian gas field (reserves of up to $8.7 \times 10^{11} \text{ m}^3$), no major oil and gas exploration breakthroughs in the southern basin have been identified during the last three decades (Liu et al., 2012; Ren et al., 2014a, 2017, 2020b; Du et al., 2019; Yang et al., 2021a, 2021c).

Exploration and research have shown that the Mesozoic strata in the southern Ordos Basin contains high-quality source rocks, reservoirs with good physical properties and an ideal source rock-reservoir accumulation condition (Chen et al., 2006, 2007; Ren et al., 2014b). The Paleozoic carbonate strata are thick (>2500 m), rich in organic matter, contain secondary dissolution pores and have reached the over-mature dry gas generation stage (Ren et al., 2014a; Du et al., 2019; Fu et al., 2019; Yang et al., 2021a, 2021c). PetroChina, Sinopec and the Yanchang Petroleum Group Co., Ltd. have conducted numerous oil and gas exploration studies in the southern Ordos Basin, which have discovered oil-gas fields in the Yichuan, Huanglong and Qingcheng areas. This shows that the southern Ordos Basin has good petroleum exploration prospects (Ren et al., 2014a, 2015, 2021; Du et al., 2019; Fu et al., 2019; Yang et al., 2021a, 2021c).

The southern Ordos Basin is located between active tectonic belts (i.e., the Tibetan Plateau, Qinling and Liupanshan orogenic belts) and a stable tectonic area (i.e., the North China Craton, Fig. 1(b)). It can be divided into five tectonic zones, including the Western Thrust Zone, Tianhuan Depression, Shaanbei Slope, Jinshaan Tectonic Zone and Weibei Uplift (Fig. 2). The southern Ordos Basin contains Proterozoic, Lower Paleozoic (Cambrian and Ordovician), Upper Paleozoic (Upper Carboniferous and Permian) and

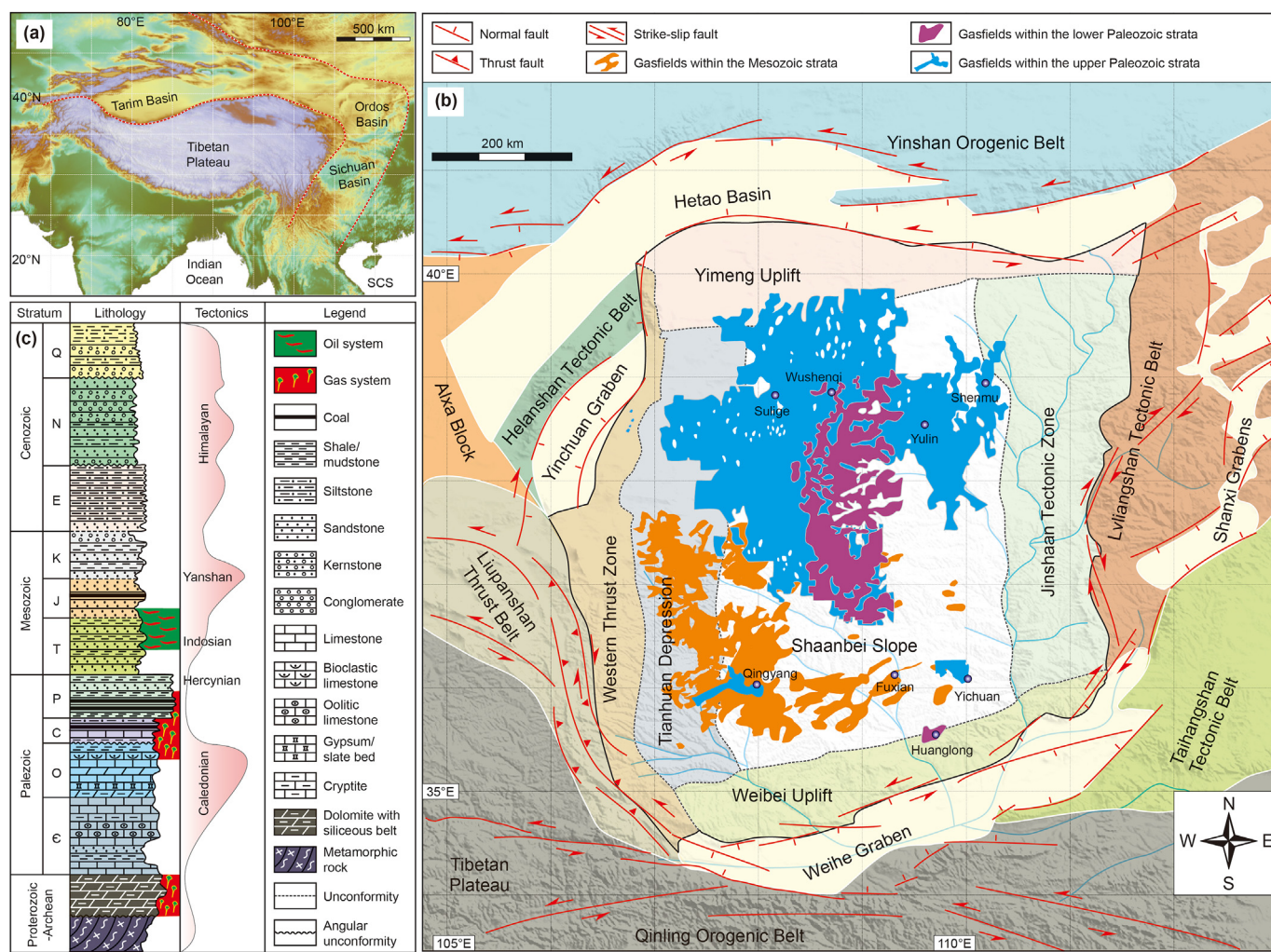


Fig. 1. (a) Location of the Ordos Basin. (b) Main tectonic units and the distribution of oil-gas fields in Ordos Basin (Fu et al., 2019; Yang et al., 2021a). (c) Stratigraphy, hydrocarbon-bearing strata and main tectonic events in Ordos Basin (Yang et al., 2021a). Abbreviation: C—Cambrian, O—Ordovician, C—Carboniferous, P—Permian, T—Triassic, J—Jurassic, K—Cretaceous, E—Paleogene, N—Neogene, Q—Quaternary.

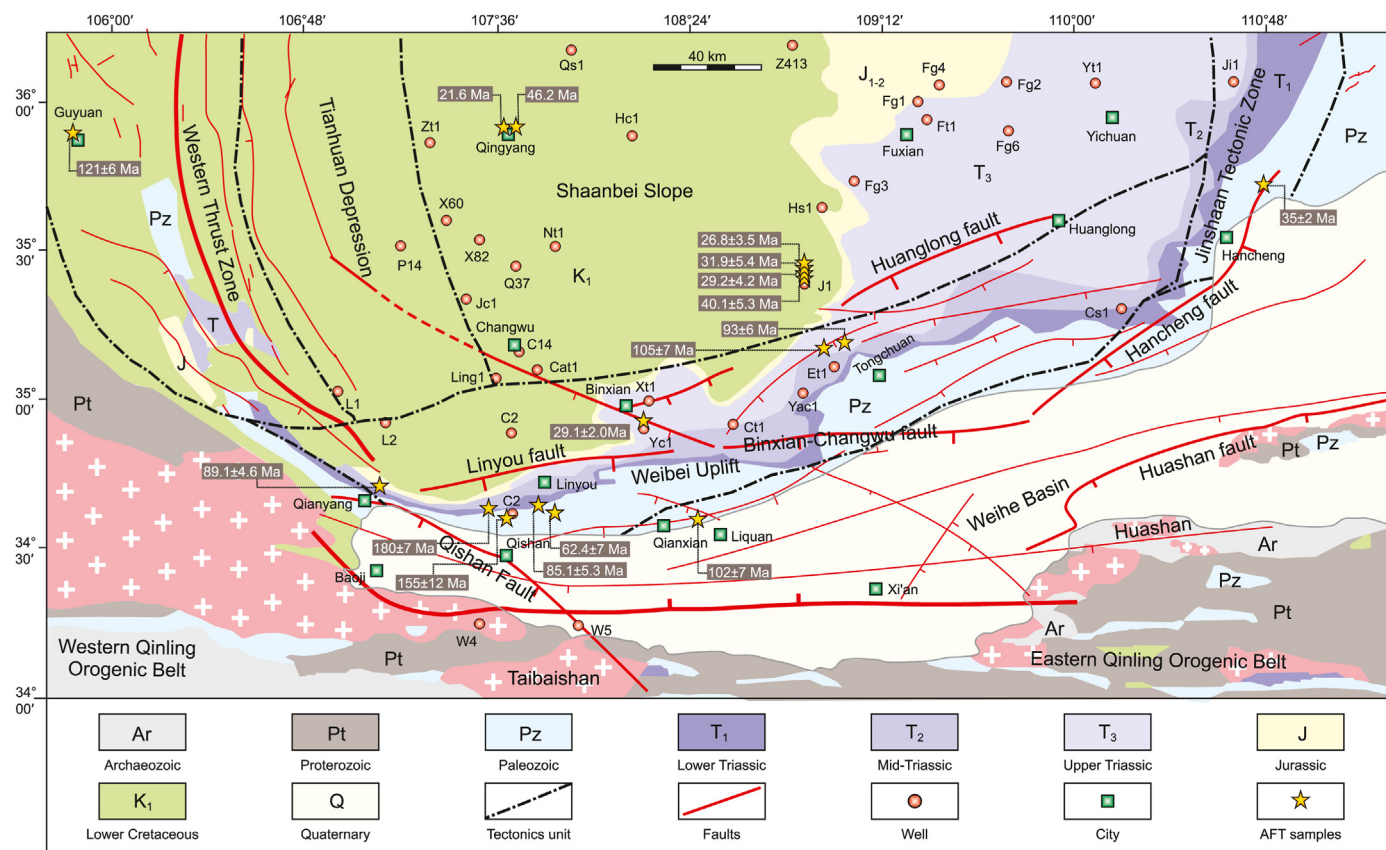


Fig. 2. Distribution of stratigraphy, fault system and apatite fission track sample's locations in the southern Ordos Basin (modified from Ren et al., 2014a, 2015; Yang et al., 2018).

Mesozoic (Triassic, Jurassic and Lower Cretaceous) strata, and lacks Silurian, Devonian, Lower Carboniferous and Upper Cretaceous strata (Fig. 2). These rocks record multiple sedimentary and tectonic cycles (Zhou et al., 1994; Yuan and Zhao, 1996a; Yuan and Wang, 1996b; Zhang et al., 2006, 2007; Yang et al., 2021a, 2021c). The multiple stages of tectonism in the southern Ordos Basin have led to a complex thermal evolution. The tectono-thermal evolution of a basin is an important controlling factor on the processes of petroleum generation and accumulation (Zuo et al., 2011, 2015; Qiu et al., 2012; Yang et al., 2020; Ren et al., 2020b, 2021). Therefore, understanding the geothermal conditions and tectono-thermal history is important for guiding deep oil and gas exploration in southern Ordos Basin (Jia and Pang, 2015; Ren et al., 2020a, 2020c).

This study integrated geochronological data and various temperature parameters, including formation-testing temperature, terrestrial heat flow, vitrinite reflectance (R_o), fission-track dating and fluid inclusions, to constrain the tectono-thermal history of the southern Ordos Basin. This work shed light on understanding the petroleum generation, accumulation and preservation condition from a novel tectono-thermal perspective, and provide important insights into future oil and gas exploration.

2. Present geothermal conditions

The present geothermal conditions provide the basis for reconstructing the paleo-geothermal gradient of a basin (Ren et al., 2007, 2014c; Zuo et al., 2011, 2015; Qiu et al., 2012; Yang et al., 2017, 2020). Based on the temperature measurement data in different areas and wells, we compiled the present geothermal conditions of Triassic, Permian and Ordovician stratum in the southern Ordos Basin (Fig. 3). In general, the temperature increases with burial

depth, but the temperature in the same strata can vary significantly in different areas.

For the Triassic strata, the temperature is mainly between 30 °C and 80 °C, with some variations in different regions. To the west of the Wuqi-Qingyang-Zhenyuan areas, the Triassic strata are deeply buried and the highest temperatures are up to 80 °C. In the southeast of the basin, the Triassic strata are shallowly buried and the temperature is only 30 °C in the Yichuan-Huanglong area (Fig. 3(a)). For the Permian strata, the temperatures are mainly 65–135 °C. The highest temperatures (>135 °C) characterize the western part of the Huanxian-Zhenyuan areas. In the Yanan-Fuxian areas, the temperatures are 95–105 °C. The lowest temperatures of 65–85 °C characterize the southeastern Yichuan-Huanglong areas (Fig. 3(b)). For the Ordovician strata, the temperatures are mainly 70–140 °C. The highest temperatures (>140 °C) characterize the northwestern part of the Zhenyuan-Huanxian areas. In the Wuqi-Zhidan areas, the temperatures are 110–130 °C. The temperatures in the Yanan-Fuxian areas are lower (90–110 °C) and in the southern Binxian-Chunhua areas are <90 °C. The lowest temperature (<80 °C) characterizes the southeastern part of Huanglong (Fig. 3(c)). The present temperatures are generally low in the southeast and high in the northwest, which is consistent with the stratigraphic frame that shallow burial in the southeast and deep burial in the northwest.

We reassessed the present geothermal gradient based on the relationship between the temperatures derived from the stratigraphy and depth. The results suggest that the geothermal gradients vary from 20 °C/km to 24 °C/km in the western Pingliang-Guyuan areas. In the Huanxian and Zhenyuan areas, the present geothermal gradients are 26–28 °C/km. In the southern Binxian-Tongchuan areas, the present geothermal gradient is <26 °C/km. In the Fuxian-

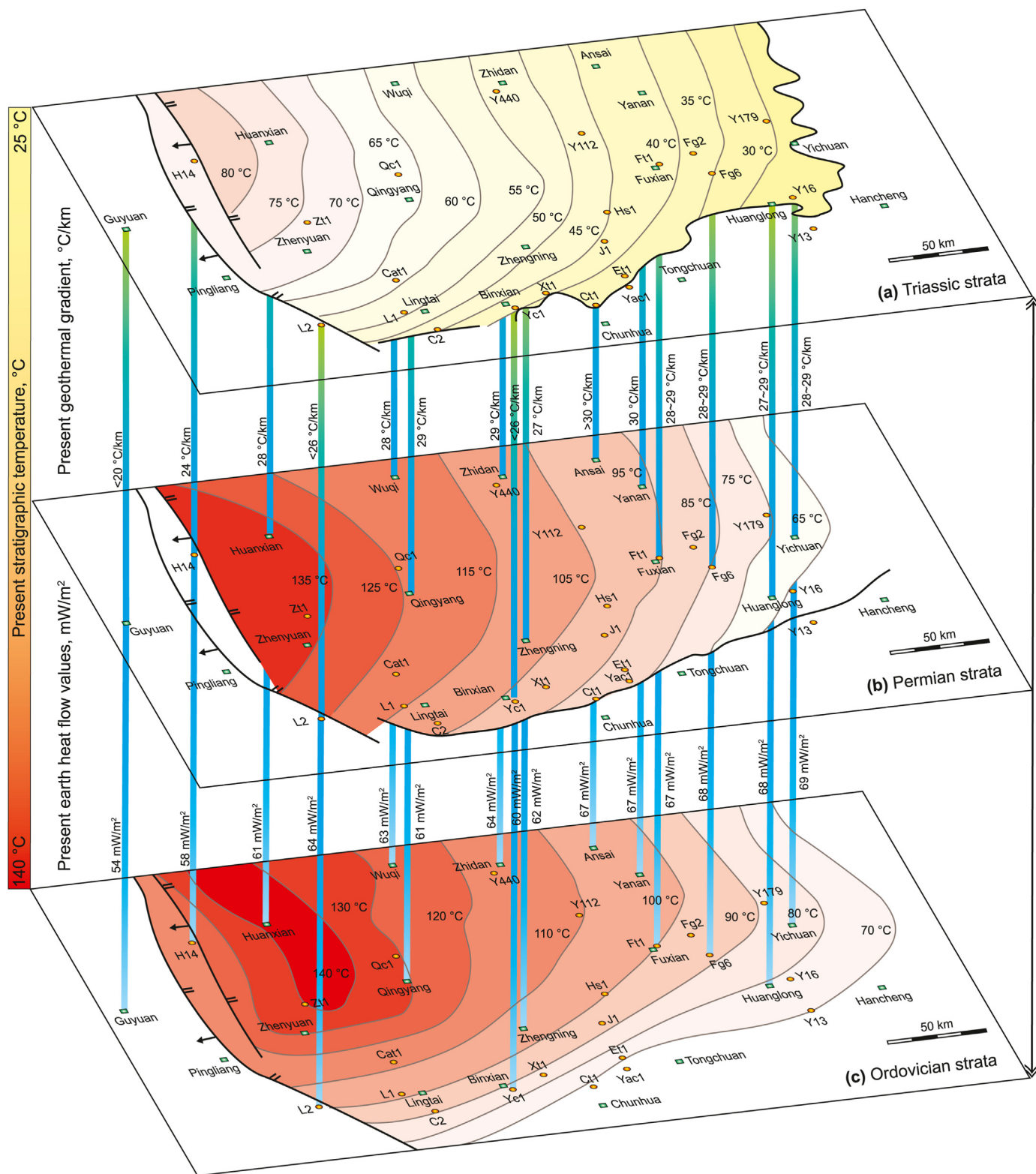


Fig. 3. Characteristics of present geothermal field in the southern Ordos Basin.

Yichuan areas, the present geothermal gradients are relatively high (28–29 °C/km). The highest present geothermal gradient (>29 °C/km) characterizes the Qingyang-Ansai-Yan'an areas (Fig. 3). Based on the present geothermal gradients and thermal conductivity, we reevaluated the heat flow features of the southern Ordos Basin

(Fig. 3). In the western Pingliang-Guyuan areas, the heat flows are relatively low (54–58 mW/m²). The heat flows are <60 mW/m² in the Binxian-Tongchuan areas and are 61–64 mW/m² in the Huanxian-Zhenyuan areas, respectively. Relatively high heat flows (64–69 mW/m²) characterize the Shaanbei Slope. The distributions

of geothermal gradients and heat flow are similar in the southern Ordos Basin.

3. Thermal maturity constrained by vitrinite reflectance

The vitrinite reflectance value (R_o) is a key indicator of thermal maturity and can be used to calculate the maximum paleo-temperature (Barker and Pawlewicz, 1986; Wang et al., 2007; Ren et al., 2014c; Yang et al., 2020). For the Triassic and Permian strata with mudstones and coal measures, the thermal maturity can be evaluated by R_o values. For the Ordovician-Cambrian carbonate strata that do not contain vitrinite, the equivalent reflectance (R_{equ}) can be obtained from the relationship between bitumen reflectance (R_b) and R_o (Jacbo, 1989; Xiao et al., 2000; Petersen et al., 2009; Qiu et al., 2012; Ren et al., 2014a, 2014c). The maximum paleo-temperatures were calculated from R_o and R_{equ} values. The value of R_o and/or R_{equ} used to indicate the stage of thermal maturity of source rocks can be classified as follows (Qiu et al., 2012; Zuo et al., 2015; Yang et al., 2020): immature ($R_o/R_{equ} < 0.5\%$), early mature ($0.5\% < R_o/R_{equ} < 0.7\%$), middle mature ($0.7\% < R_o/R_{equ} < 1.0\%$), late mature ($1.0\% < R_o/R_{equ} < 1.3\%$), main gas stage ($1.3\% < R_o/R_{equ} < 2.0\%$), dry-gas stage ($R_o/R_{equ} > 2.0\%$). Based on this, we determined the thermal maturity of the Triassic, Permian and Ordovician strata in the southern Ordos Basin (Fig. 4). As the burial depth increases and the strata become older, the R_o and/or R_{equ} values increase and the thermal maturity increases. However, R_o and/or R_{equ} values for a given formation vary significantly in different regions of the southern Ordos Basin.

For the Triassic strata, R_o values are $>0.7\%$ and the thermal maturity has reached the middle-mature oil generation stage. The R_o values in the western part of the southern Ordos Basin range from 0.7% to 0.8% and the thermal maturity is lower than elsewhere. The R_o values in the Qishan-Yongshou-Binxian-Xunyi areas in the southwestern basin range from 0.8% to 0.9%, indicative of a relatively high degree of thermal maturity. The R_o values in the Tongchuan-Chengcheng-Huanglong areas, in the southeastern Ordos Basin, range from 0.7% to 0.9%. The R_o values in the eastern Hancheng-Hejin areas are $\sim 0.7\%$. From the Qingyang-Ningxian-Zhengning-Fuxian-Heshui areas towards the interior of the basin, R_o values increase up to maximum values of 1.0%. In the Fuxian-Heshui areas, the R_o values are $>1.0\%$, indicative of the late-mature oil generation stage (Fig. 4a).

For the Permian strata, most of R_o values are $>2.0\%$ and the thermal maturity has reached the over-mature dry gas generation stage as a whole. However, the R_o values of the Permian strata are variable in different areas. In the west, the R_o value of Permian strata in Well L2 is 1.92% and the thermal evolution caused that kerogen reached main gas generation stage. The R_o values of Permian strata are relatively high in the Qishan-Yongshou-Binxian-Xunyi areas on the southwestern margin of the Weibei Uplift. The R_o values of Well C2 and Well Ct1 are 2.07%–2.10%. In the Tongchuan-Chengcheng-Huanglong areas of the eastern part of the Weibei Uplift, the R_o values are 1.8%–2.0%. In the Hancheng-Hejin areas of the southeastern Ordos Basin, the R_o values are $<1.8\%$. The R_o values and thermal evolution increase gradually from the basin margin to central part of basin. The R_o values of Permian strata in Well Ft1 are up to 2.81%, which are indicative of the over-mature dry gas generation stage (Fig. 4(b)).

Vast majority of R_o values of Ordovician strata in the southern Ordos Basin are $>2.0\%$ and the thermal maturity has reached the over-mature dry gas generation stage. In the Qishan-Yongshou-Binxian-Xunyi areas at the southwestern margin of the basin, the R_o values are 2.0%–2.5%, indicative of a relatively high degree of thermal maturity. In the Tongchuan-Chengcheng-Huanglong areas in the southeastern Ordos Basin, the R_o values are 1.8%–2.0%. The

lowest R_o values ($<1.8\%$), indicative of the over-mature dry gas generation stage, characterize the Hancheng-Hejin areas in the Jinshaan Tectonic Zone in the southeastern Ordos Basin. From the margins of the basin to the Shaanbei Slope in the inner part of the basin, R_o values increase up to a maximum of $>3.0\%$ (Fig. 4(c)). The highest thermal evolution characterizes the Qingyang-Ningxian-Zhengning-Fuxian-Heshui areas.

In the southern Ordos Basin, the Triassic to Ordovician strata have different maturities and have reached variable oil and gas generation stages. As such, the maturity controls the oil and gas distribution. The R_o values of the Triassic strata are low (0.7%–1.16%). The thermal evolution caused that kerogen from the Triassic source rock reached the middle-mature to late-mature liquid oil generation stage. The R_o values of the Permian and Ordovician strata are higher ($>1.8\%$), indicative of the over-mature dry gas generation stage.

4. Time-temperature history constrained by apatite fission-track dating

To constrain the time-temperature history of the southern Ordos Basin, we collected apatite fission-track (AFT) ages for Cambrian (sample Xbf-3), Ordovician (samples Lyb-1 and Dz-5), Permian (samples Qsc-13 and Lyb-2), Triassic (sample Qsf-1), Triassic (samples J1-1, J1-3, J1-6, Zh39-5, Yc-1, Tns-1, Tns-3, Qy-lx01 and Gy-ts1) and Jurassic (sample Zh39-1) strata. The details of the method descriptions and the AFT dataset provided in the supplementary information. The oldest AFT ages (180 ± 7 Ma and 155 ± 12 Ma) characterize the Qishan area along the southwestern margin of the Ordos Basin. The AFT ages in the western Guyuan and Qianyang areas are 121 ± 6 Ma and 89.1 ± 4.6 Ma, respectively. The AFT ages in the southern Qianxian area are 102 ± 7 Ma, 105 ± 7 Ma and 93 ± 6 Ma and the AFT ages in the Linyou area are 85.1 ± 5.3 Ma and 62.4 ± 3.6 Ma. These ages are much older than those of Well Yc1 in the northern Binxian area (29.1 ± 2.0 Ma), the Qingyang area (21.6 Ma and 46.2 Ma), Well J1 (26.8 ± 3.5 Ma, 31.9 ± 5.4 Ma, 29.2 ± 4.2 Ma and 40.1 ± 5.3 Ma) and the Hancheng-Xiabaifan areas (35 ± 2 Ma, Figs. 2 and 5). All the AFT ages are younger than the stratigraphic ages and the fission-track lengths vary from 10.4 ± 2.6 μm to 13.03 ± 1.63 μm (Fig. 5), which are significantly shorter than the initial lengths (16.3 ± 0.9 μm , Gleadow et al., 1986). Therefore, all the samples have undergone significant fission-track annealing and the results cannot be used to research the evolution of the orogenic belt in the provenance area. However, the ages can constrain the uplift, exhumation and tectono-thermal history of the basin.

In this study, we reconstructed a time-temperature history using the fission-track data for the southern Ordos Basin via HeFTy software (Ketcham, 2005; Fig. 6). The age GOF (goodness of fit between model and measured value) range from 0.93 to 0.99 and the length GOF range from 0.57 to 0.99 (Table S1), which are larger than the 0.50 suggesting the reconstructed thermal histories are reliable. The time-temperature history of the Permian sample Qsc-13 revealed a heating stage before 215 Ma in the southwestern basin and a maximum paleo-temperature was reached at 215 Ma. This may indicate a tectono-thermal event at 215 Ma (Yang et al., 2021c), followed by large-scale uplift and cooling (Fig. 6). During this period, a Late Triassic collisional orogeny and granitic magmatism in the Qinling area ended at the periphery of the basin and the southern Ordos Basin began to enter a stage of intracontinental tectonism (Zhang et al., 2005, 2008; Wang et al., 2015; Dong et al., 2016). This may have caused uplift and faulting in the Western Thrust Zone (Wang et al., 2020). The sediment provenance of the southwestern Ordos Basin is mainly the eastern Qilian Mountains and initial uplift and exhumation of the eastern Qilian Mountains

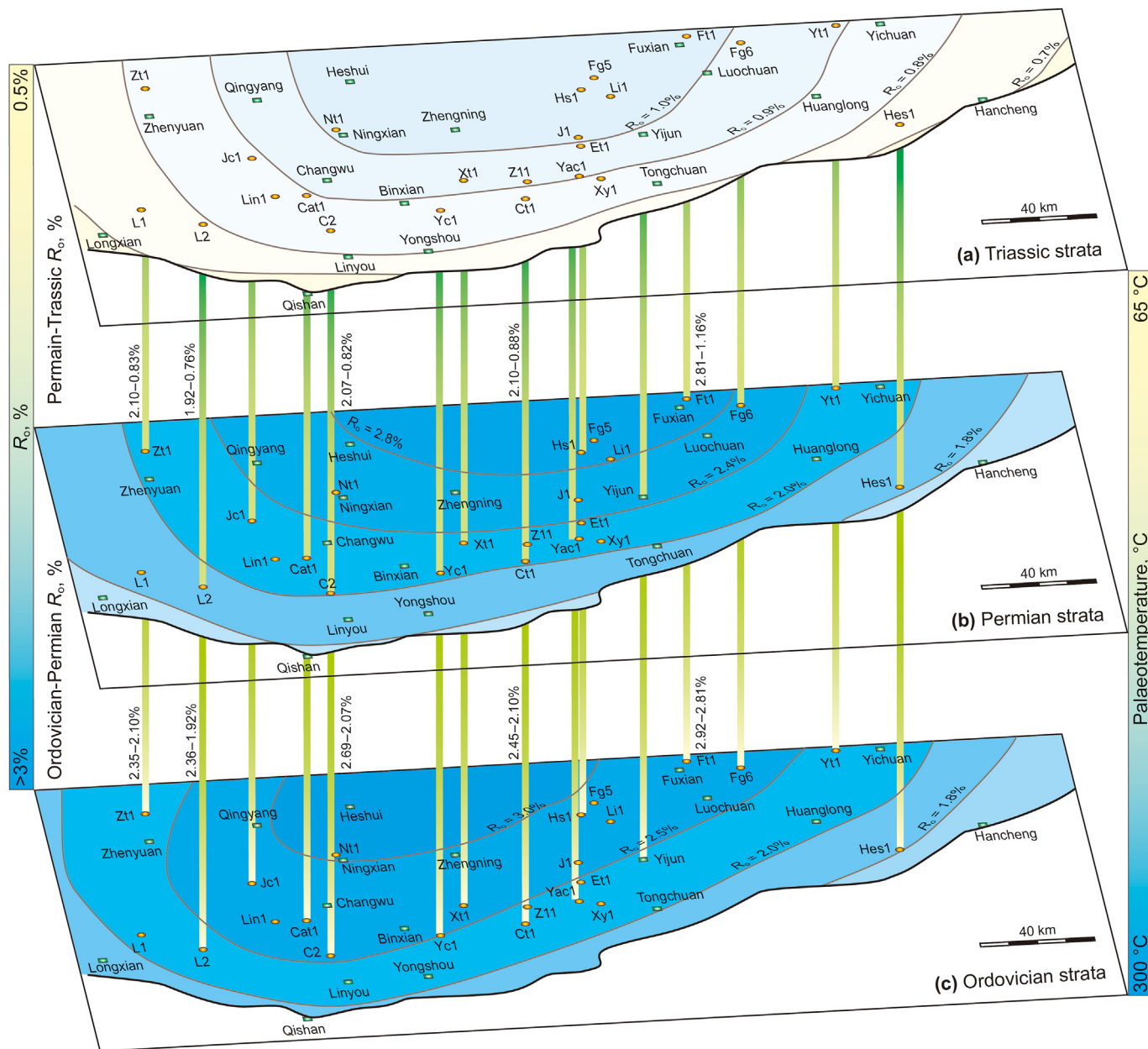


Fig. 4. Distribution of the thermal maturity constrained by vitrinite reflectance in southern Ordos Basin. (a) Triassic strata, (b) Permian strata, (c) Ordovician strata.

occurred at ca. 215 Ma (Peng et al., 2018). This indicates that the timing of large-scale uplift and denudation in the southwestern basin was younger than 215 Ma. The R_0 values of Jurassic and Triassic strata in the southwestern basin exhibit a linear relationship with depth (Ren et al., 2007, 2014a, 2015; Yang et al., 2021c), which indicates there is no paleo-geothermal gradient unconformity between the Jurassic and Triassic strata, or that the scale of this tectono-thermal event was limited. It is unlikely that a large-scale tectono-thermal event occurred during the Hercynian-Indosinian orogenies. The southern Ordos Basin was in lacustrine and swamp facies during the Hercynian-Indosinian periods. These sedimentary facies and a fault-related calcite U–Pb age of 214 Ma for this area (Yang et al., 2021c) suggest the 215 Ma tectono-thermal event was related to localized fault activity caused by Indosinian intracontinental deformation.

The regional angular unconformity between Jurassic and Lower

Cretaceous strata in the southern Ordos Basin indicates that regional uplift and denudation occurred during the Yanshanian orogeny in the Late Jurassic. The time-temperature paths of samples Gy-ts1 (Guyuan area), Qsf-1 (Qishan area) and Dz-5 (Liquan-Dongzhuang areas) reveal that uplift and cooling occurred at 165–150 Ma in the Late Jurassic along the southern and western margins of the Ordos Basin (Fig. 6). The time-temperature paths of samples from the Qianyang (Qy-lx01), Linyou (Lyb-1 and Lyb-2), Tongchuan (Tns-1 and Tns-5) and Qingyang (Zh39-1, Zh39-5) areas indicate that the southern basin reached a maximum paleo-temperature during 120–110 Ma and then experienced large-scale uplift and exhumation (Fig. 6). The time-temperature paths of samples from Well Yc 1 (Yc-1) and the Liquan-Dongzhuang (Dz-5) and Well J1 (J1-1, J1-3 and J1-6) show that the southern Ordos Basin reached a maximum paleo-temperature at 110–100 Ma (Fig. 6).

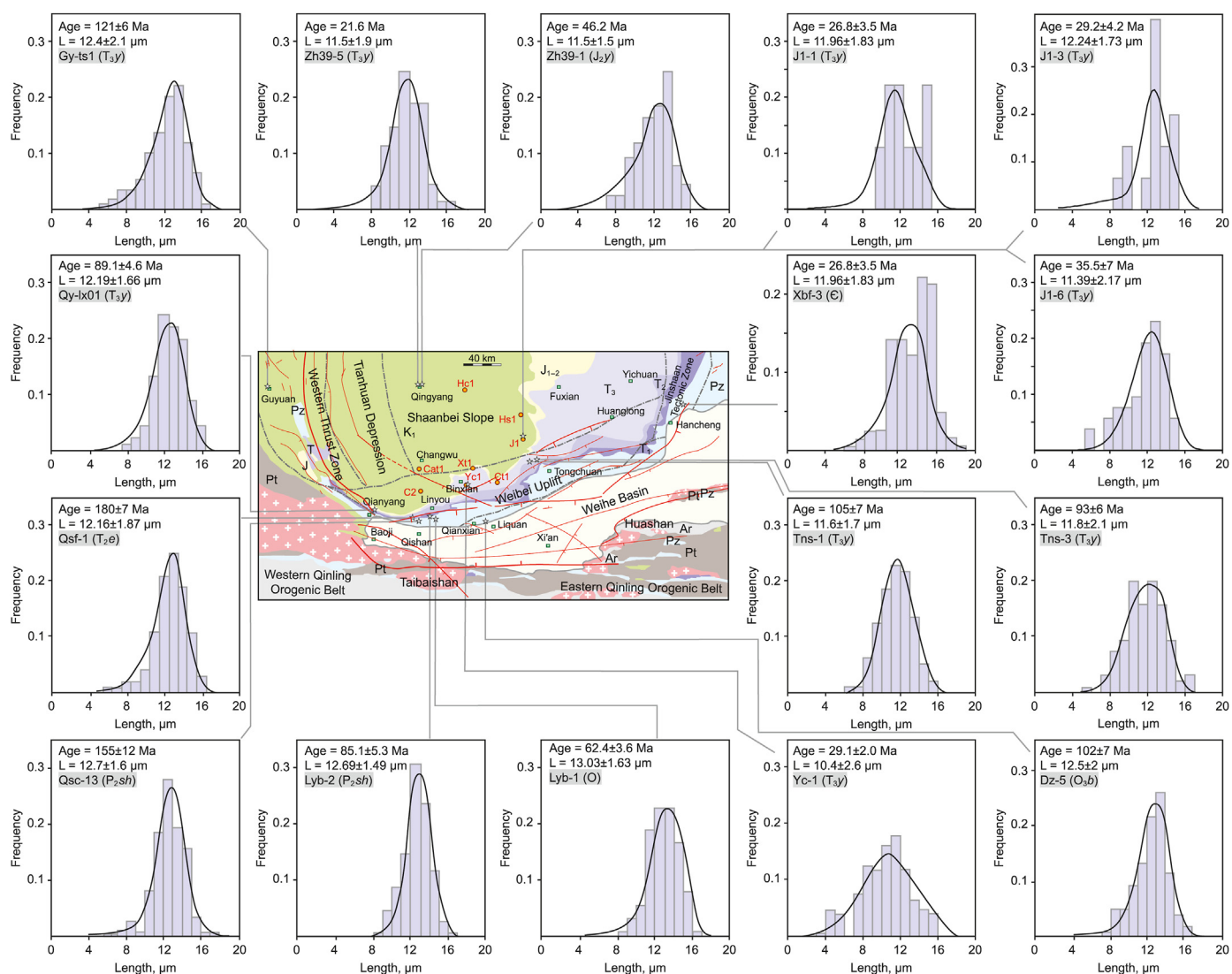


Fig. 5. Apatite fission track ages and length in the southern Ordos Basin. (Samples Yc-1 from Ren, 1995; Zhao et al., 2018; Gy-ts1 from Song et al., 2013; Qsc-13 from Ren et al., 2014a; Zh39-1 and Zh39-5 from Lei, 2015; Tns-1 and Tns-3 from Xu et al., 2017; Qsf-1 from Yu et al., 2019; Qy-lx01 from Yu et al., 2021; samples J1-1, J1-3, J1-6, Xbf-3, Dz-5, Lyb-1 and Lyb-2 are from this study).

During the Yanshanian orogeny, the southern Ordos Basin experienced intense deformation related to the Qinling orogenic belt to the south and Liupanshan Thrust Belt to the west. These processes generated thrust structures in the southern Ordos Basin, which deformed the pre-Jurassic strata (Yang et al., 2021a). The Late Jurassic (165–150 Ma) events occurred mainly at the margin of the Western Thrust Zone and southern margin of the Weibei Uplift. At ca. 120 Ma, the Yanshanian orogeny began to affect the Shaanbei Slope in the basin interior. At the end of the Early Cretaceous (ca. 110 Ma), the southern Ordos Basin began to experience large-scale cooling. During the Late Cretaceous and Cenozoic, the southern Ordos Basin underwent continuous uplift and cooling. Rapid uplift and significant cooling have occurred since 40 Ma, with accelerated uplift and cooling since 20–10 Ma (Fig. 6). The time-temperature paths indicate three stages of Mesozoic tectonism in the southern Ordos Basin, which were in the Triassic (ca. 215 Ma), Late Jurassic (165–160 Ma) and End-Early Cretaceous (110–100 Ma). The main tectono-thermal event occurred at the end of the Early Cretaceous, which was widespread and had a significant effect on the thermal maturity of source rocks in the southern Ordos Basin.

5. Thermal maturity of source rocks constrained by tectono-thermal history

The southern Ordos Basin is part of the North China Craton and its crystalline basement rocks formed in the Archean-Early Proterozoic (Zhu et al., 2011b; Zhai, 2011; 2012). Due to the breakup of Rodinia and opening of the Qinling Trough, the southern basin developed Meso-Neoproterozoic to Cambrian strata (Zhai, 2012; Zhao et al., 2018). Since the Cambrian, the southern basin has experienced multiple tectonic events, such as the Caledonian, Hercynian, Indosinian, Yanshanian and Himalayan orogenies (Fig. 7, He, 2003; Yang et al., 2006, 2018, 2021c).

From the Early Cambrian to Early-Middle Ordovician during the Caledonian Orogeny, apart from the area around the Qingyang paleo-uplift (Well Zt1, Fig. 7), most areas of the southern basin were still undergoing subsidence (Fig. 7), during which Cambrian-Ordovician source rocks were deposited (Zhu et al., 2011a). During the Middle-Late Caledonian Orogeny period, the southern Ordos Basin experienced orogenesis that formed a series of thrust nappe structures and folds. The deformation intensity gradually

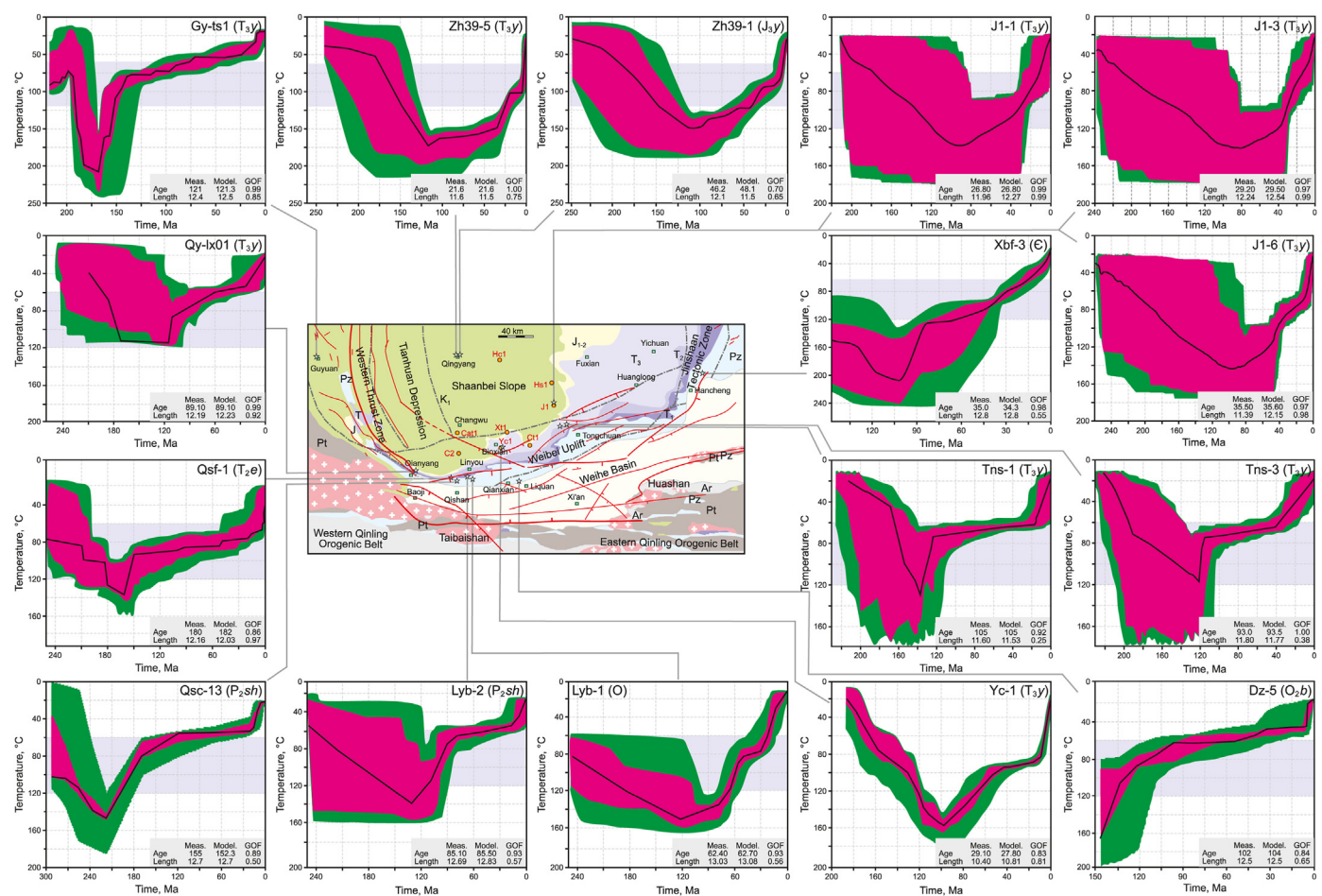


Fig. 6. Modeled time-temperature curves based on the results of apatite fission track dating in the southern Ordos Basin. (Samples Gy-ts1 from Song et al., 2013; Zh39-1 and Zh39-5 from Lei, 2015; samples Xbf-3 and Dz-5 from Ren et al., 2015; Tns-1 and Tns-3 from Xu et al., 2017; Yc-1 from Yu et al., 2018; Qsf-1 and Qsc-13 from Yu et al., 2019; Qy-lx01 from Yu et al., 2021; samples J1-1, J1-3, J1-6, Lyb-1 and Lyb-2 are from this study).

weakened from the basin margin to interior, which was associated with subduction in and closure of the ancient Qinling and Proto-Tethyan oceans (Zhou et al., 1994; Yuan and Wang, 1996b; Yuan and Zhao, 1996a; Zhang et al., 2006, 2007; Yang et al., 2021a, 2021c). The Upper Paleozoic strata are separated by an angular unconformity from Lower Paleozoic strata (Yuan and Wang, 1996b; Yuan and Zhao, 1996a; Yang et al., 2021a). This event may be recorded by fault-related carbonate with a U–Pb age of 452 Ma (Yang et al., 2021c). The southern part of the basin was uplifted during the Caledonian Orogeny (Fig. 7). The Caledonian tectonism prevented the Paleozoic source rocks from experiencing rapid burial and heating. Given the rapid burial and heating of source rocks in the eastern Tarim Basin during the Early Paleozoic, the maturity of source rocks in the southern Ordos Basin differs significantly from those in the eastern Tarim Basin (Qiu et al., 2012; Yang et al., 2021b). Organic matter in source rocks is continuously transformed into hydrocarbons and the residual organic matter in the source rocks decreases with increasing maturity (Tissot and Welte, 1978; Fang, 1986; Pang et al., 1988; Wang et al., 2019). The Caledonian Orogeny prevented the Lower Paleozoic source rocks in the southern Ordos Basin from reaching high maturity during the Early Paleozoic, which led to the Cambrian-Ordovician source rocks undergoing later hydrocarbon generation.

During the Hercynian-Indosinian orogenies, the southern Ordos Basin evolved into an intracontinental stage. During this stage,

intracontinental deformation caused faulting at ca. 214 Ma, which resulted in localized tectono-thermal events (Figs. 6 and 7; sample Qsc-13, Yang et al., 2021c). However, the burial history shows that rapid subsidence occurred during this period (Fig. 5). In addition, based on the widespread development of Paleozoic and Triassic strata, well preserved Middle-Lower Jurassic lacustrine- and swamp-facies coal beds and the linear relationship between R_0 values and depth (Ren et al., 2007, 2014a, 2015; Yang et al., 2021c), we suggest that the southern Ordos Basin was dominated by burial and heating during the Hercynian-Indosinian orogenies. Uplift, cooling and denudation were limited, which is consistent with the burial history reconstructed from wells in the southern basin (Fig. 7, Yang et al., 2021c). During the Hercynian-Indosinian orogenies, the southern Ordos Basin was dominated by subsidence and this was an important period of sedimentation of Triassic hydrocarbon source rocks. At the same time, the Paleozoic source rocks experienced burial and heating, the maturity increased and caused kerogen reached the mature hydrocarbon generation stage. This continuous burial process created favorable prerequisites for reaching the maximum paleo-temperatures in the later stage.

The Yanshanian Orogeny was an important event in the Ordos Basin and caused a major transformation in the tectonism. In particular, the Qinling orogenic belt affected the southern Ordos Basin, which led to uplift. During this stage, numerous compressional thrust belts formed in the southern part of the basin and

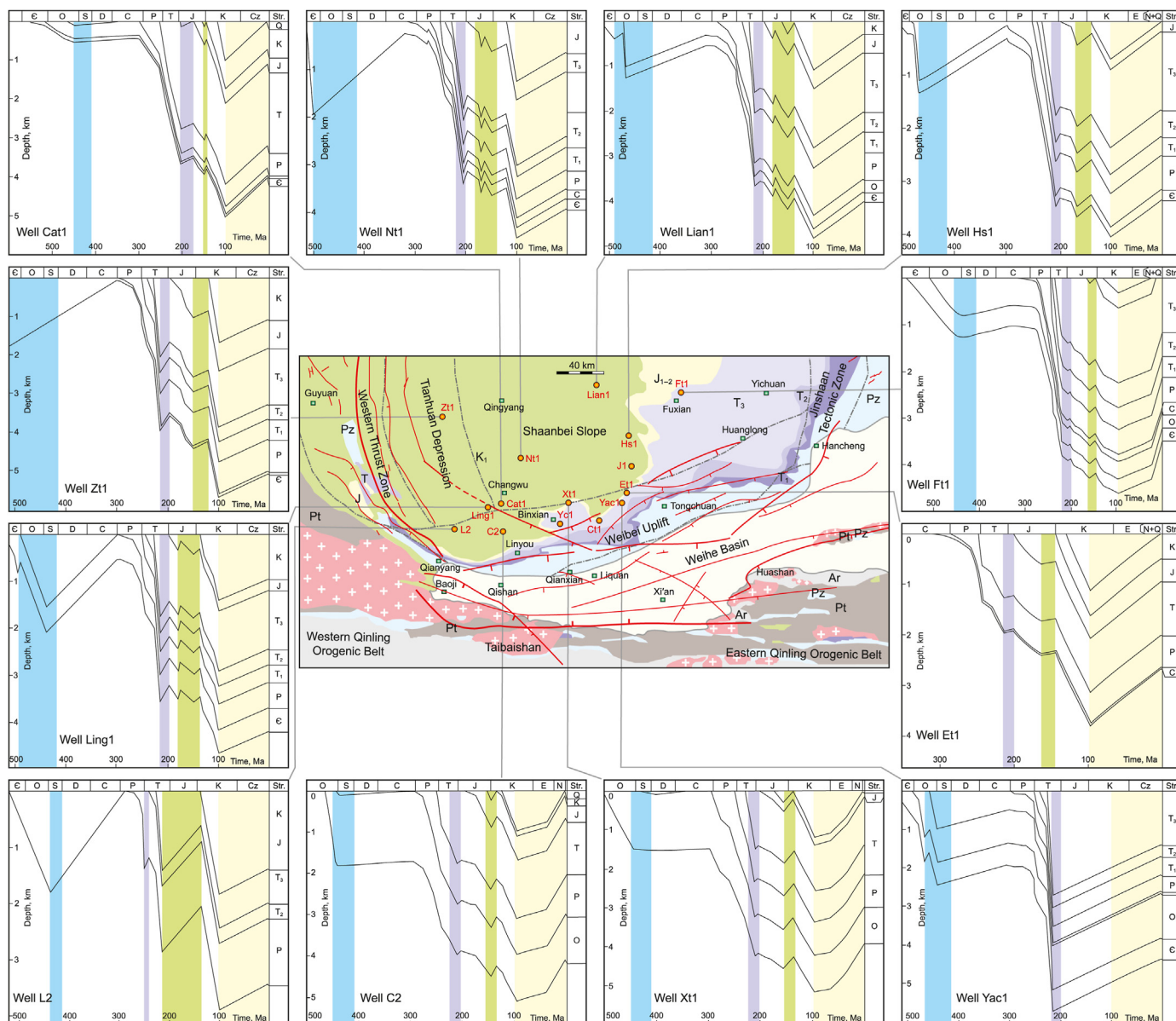


Fig. 7. Tectonic uplift and subsidence revealed by the burial histories in different tectonic units in the southern Ordos Basin.

surrounding areas (Yang et al., 2021a). The deformation was strong in the south and weak in the north. A series of anticlines and large-scale, south-dipping, northward-thrusting fault structures formed imbricate fault zones (Zhou et al., 1994; Yuan and Zhao, 1996a; 1996b; Zhang et al., 2006, 2007; Ren et al., 2014a, 2015; Yang et al., 2021a, 2021c). In addition to the well-developed folds and faults in the southern basin, the pre-Jurassic strata were folded and deformed and are unconformably overlain by Upper Cretaceous strata. Cenozoic strata are absent in the basin, which is consistent with the southern basin reaching its maximum burial depth at the end of the Early Cretaceous, followed by large-scale uplift and erosion (Ren et al., 2007, 2014a, 2015; Xiao et al., 2013; Yang et al., 2021a). The R_0 values of pre-Cretaceous strata from several wells (C2, Xt1, Ft1 and Ct1) in the southern basin exhibit a linear relationship with depth (Ren et al., 2007, 2014a; Yang et al., 2021a). This indicates that the southern basin was mainly undergoing heating prior to the Early Cretaceous and then reached its maximum burial

depth and highest paleo-temperature at the End-Early Cretaceous. The tectono-thermal event that occurred at the End-Early Cretaceous had the largest effect on the hydrocarbon source rock maturity in the southern Ordos Basin.

Since the Late Cretaceous, the southern Ordos Basin has been affected by compression in the Qinling orogenic and Liupanshan structural belts, which resulted in large-scale uplift and denudation of >2200 m (Yang et al., 2021a). During the Himalayan Orogeny, the far-field extensional effects of the northeastern margin of the Tibetan Plateau and formation of the Weihe graben resulted in southern Ordos Basin experienced accelerating uplift and denudation (Ren, 1995; Sun and Liu, 1996; Ren et al., 2014a, 2015; Yang, 2002; Zhang et al., 2006; Xiao et al., 2013; Yang et al., 2018, 2021a, 2021c). The southern part of the basin has been dominated by uplift and cooling during the Late Cretaceous and the Cenozoic period, which made little contribution to the increasing thermal maturity of the Cambrian-Ordovician and Triassic source rocks.

6. Implications for petroleum generation, accumulation and preservation

The southern Ordos Basin was dominated by burial and heating during the Cambrian and experienced cooling caused by uplift and denudation during the Caledonian Orogeny. During the Late Carboniferous–Early Permian, the basin was dominated by rapid subsidence and heating. Until the end of the Cretaceous, the southern Ordos Basin reached a maximum burial depth at ca. 110 Ma. The maximum paleo-temperatures were generally $>200\text{ }^{\circ}\text{C}$ and exceeded $240\text{ }^{\circ}\text{C}$ in some areas. The maximum paleo-temperatures in the south were significantly higher than those in the north ($160\text{ }^{\circ}\text{C}$ in Well Sc1). Since the Late Cretaceous, the southern Ordos Basin again experienced uplift and cooling, which increased further during the Cenozoic (Fig. 8(a)–(e)). The heat flow also increased significantly in the Early Cretaceous (Fig. 8(f)), indicative of a tectono-thermal event. At the End–Early Cretaceous, the heat flow in the Weibei Uplift in the southern basin was higher than that in the Shaanbei Slope in the northern basin and exhibits an inverse relationship with lithospheric thickness. In the Tianhuan Depression and Western Thrust Zone, the Cretaceous heat flow was lowest but the lithospheric thickness was greatest (Fig. 8(f)). Given that this tectono-thermal event in the southern Ordos Basin occurred during thinning and destruction of the North China Craton, we suggest that the Cretaceous tectono-thermal history was controlled by the thermal structure of the deep lithosphere. Destruction of the North China Craton had an important role in controlling the tectono-thermal evolution of the Qinshui Basin adjacent to the eastern margin of the Ordos Basin (Liu et al., 2021). The thinning and destruction of the North China Craton at the End–Early Cretaceous may have also affected the geothermal gradient in the southern Ordos Basin. This is consistent with the Moho depth being shallow in the southern Ordos Basin and deeper to the north, and the thickness of the lithosphere being thinner in the south and thicker to the north (Ren et al., 2020b).

The tectono-thermal history of a basin controls petroleum generation. Triassic source rocks in the southern Ordos Basin began to generate petroleum during the Jurassic. The maximum paleo-temperatures occurred at the End–Early Cretaceous, which were up to $160\text{ }^{\circ}\text{C}$. At this time, the Triassic source rocks entered the late mature stage and began to generate petroleum. The Carboniferous–Permian source rocks began to generate petroleum during the Triassic. The rapid subsidence and heating during this stage caused coal measure-type source rocks to enter the mature oil generation stage in the Triassic and gas generation stage in the Late Jurassic. At the End–Early Cretaceous, the Carboniferous–Permian source rocks reached the peak of the gas generation stage. The Cambrian–Ordovician carbonate source rocks began to generate petroleum during the Permian, then entered the mature oil generation stage during the Late Triassic, and subsequently reached the peak stage of natural gas generation during the end–Cretaceous (Fig. 8(a)–(e)).

On the other hand, the previous results of illite K–Ar and $^{40}\text{Ar}/^{39}\text{Ar}$ dating suggested that petroleum accumulation in the Mesozoic reservoirs mainly developed during the Early Cretaceous (117.2–95.6 Ma, Li and Ren, 2010; Ren et al., 2014b; Ren and Liang, 2010). Fluid inclusion studies of the Yanchang Formation in the Zichang and Fuxian–Zhengning areas, combined with the tectono-thermal history, also suggest that petroleum accumulation developed mainly during the Early Cretaceous (120–100 Ma) in Mesozoic reservoirs in the southern Ordos Basin (Liang et al., 2011a, 2011b). This inference is also supported by results obtained from reservoir saturation pressure methods, which show that petroleum accumulation occurred mainly during the Early Cretaceous (Li and Ren, 2010; Ren and Liang, 2010). Illite dating of Carboniferous–Permian strata (i.e., the Shihezi, Shanxi and Taiyuan formations)

also shows that petroleum accumulation developed mainly during 110–100 Ma (Ren et al., 2020b). Therefore, the main period of oil and gas accumulation in Upper Paleozoic strata was at the End–Early Cretaceous (Liu et al., 2005). In addition, the thermal history of Lower Paleozoic strata in multiple wells suggests that petroleum accumulation in Cambrian–Ordovician strata also occurred during the Early Cretaceous (Ren et al., 2014a, 2017, 2020b, 2021).

In the southern Ordos Basin, the timing of petroleum generation and accumulation in Mesozoic and Paleozoic strata was mainly in the Early Cretaceous, which coincides with the timing of destruction and thinning of the North China Craton, a tectono-thermal event and the maximum paleo-temperatures and geothermal gradients (Ren et al., 2007, 2014b, 2017, 2020b, 2021). In addition, petroleum, oil shale, uranium ore and coal deposits in the southern Ordos Basin were formed during the Early Cretaceous (Ren, 1995; Ren et al., 2007, 2014a, 2014b, 2015, 2017, 2020b, 2021; Li and Ren, 2010; Chen et al., 2022). It is noted that the Au and Mo ores in the periphery of the southern basin were also formed during the Early Cretaceous (Shi and Liu, 1999; Mao et al., 2003; Zhu et al., 2008, 2009; Xiong et al., 2019). This large-scale mineralization event was not solely controlled by burial and heating or localized fault activity. Based on the inverse correlation between the regional lithospheric thermal structure and heat flow, the large-scale petroleum accumulation and mineralization during the Early Cretaceous was likely controlled by deep processes, including lithospheric extension, thinning and destruction. The deep thermal structure controlled the petroleum generation and accumulation, as it affected the tectono-thermal history of the sedimentary basin. Oil and gas generation and accumulation in the southern Ordos Basin is one of the most important shallow responses to these deep lithospheric changes.

Multiple sets of source rocks in the southern Ordos Basin did not reach the large-scale petroleum generation and accumulation stages in the Caledonian and Hercynian–Indosinian orogenies. Depleted $\delta^{13}\text{C}_{\text{carb}}$ excursions (i.e., a shift to more negative values) suggest that large-scale petroleum generation occurred in the Ordovician Formation in the Ordos Basin (Li et al., 2021). Based on the tectono-thermal evolution and hydrocarbon generation history of multiple wells, the southern Ordos Basin had petroleum generation and accumulation conditions in the Early Cretaceous that led to the formation of large-scale oil and gas reservoirs. The southern basin experienced multiple stages of tectonism during the Caledonian, Hercynian–Indosinian, Yanshanian and Himalayan orogenies, which formed fault systems and complicated the oil and gas preservation conditions (Fig. 9). Given that no major oil and gas finds have been made in the southern Ordos Basin, the large-scale uplift, denudation and faulting may have degraded the petroleum preservation conditions since the End–Early Cretaceous.

Since the Late Cretaceous, the southern part of the basin has experienced large-scale uplift and denudation and Lower Paleozoic rocks are now exposed at the surface. The Yanshanian Orogeny occurred from the basin margin to interior during the Cretaceous and advanced from south to north. Field and geophysical evidence show that deformation was stronger in the southern part of the basin than in the basin interior and this established the present structural framework of the basin (Yang et al., 2021a). This, and the greater denudation in the south than the north, along with the south-dipping and northward-thrusting faults (Yang et al., 2021a), suggests that the faults segmented the basin and affected the oil and gas preservation conditions. To the west of the Guyuan–Longxian Fault in the Western Thrust Zone and to the south of the Tianjiazui and Laolongshan faults in the Weibei Uplift, late basin transformation due to tectonism led to early uplift and extensive denudation. Cambrian–Ordovician strata crop out at the surface and/or are directly covered by Quaternary rocks. These areas have

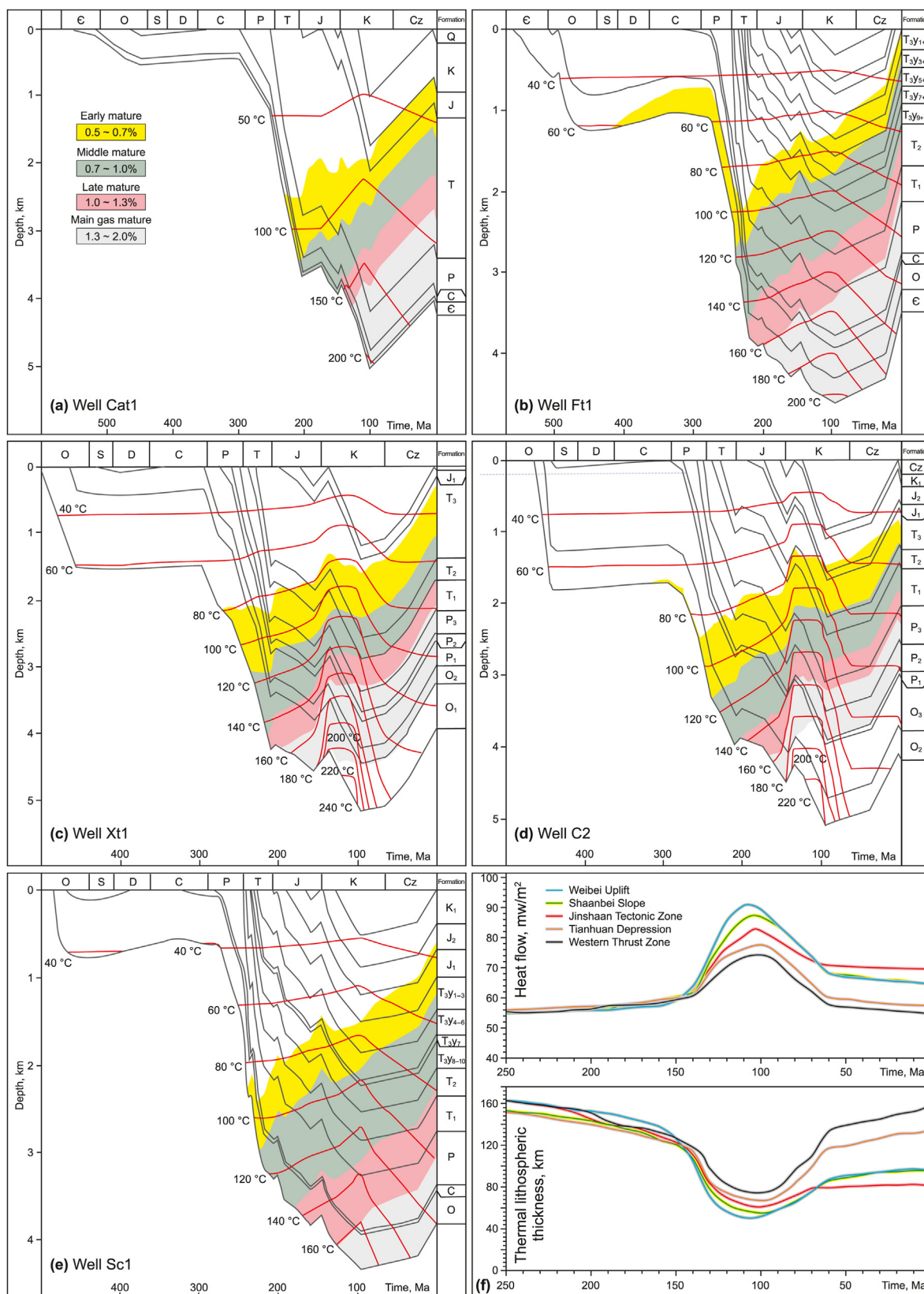


Fig. 8. Relationship between tectono-thermal evolution history and hydrocarbon generation in the Ordos Basin. (a) Well Cat1 (this study), (b) Well Ft1 (Ren et al., 2017; Yang et al., 2021a), (c) Well Xt1 (Yang et al., 2021a), (d) Well C2 (Ren et al., 2014a), (e) Well Sc1 (Ren et al., 2017; Yang et al., 2021a); (f) evolution history of heat flow and thermal lithospheric thickness of the southern Ordos Basin (Ren et al., 2020b, 2021).

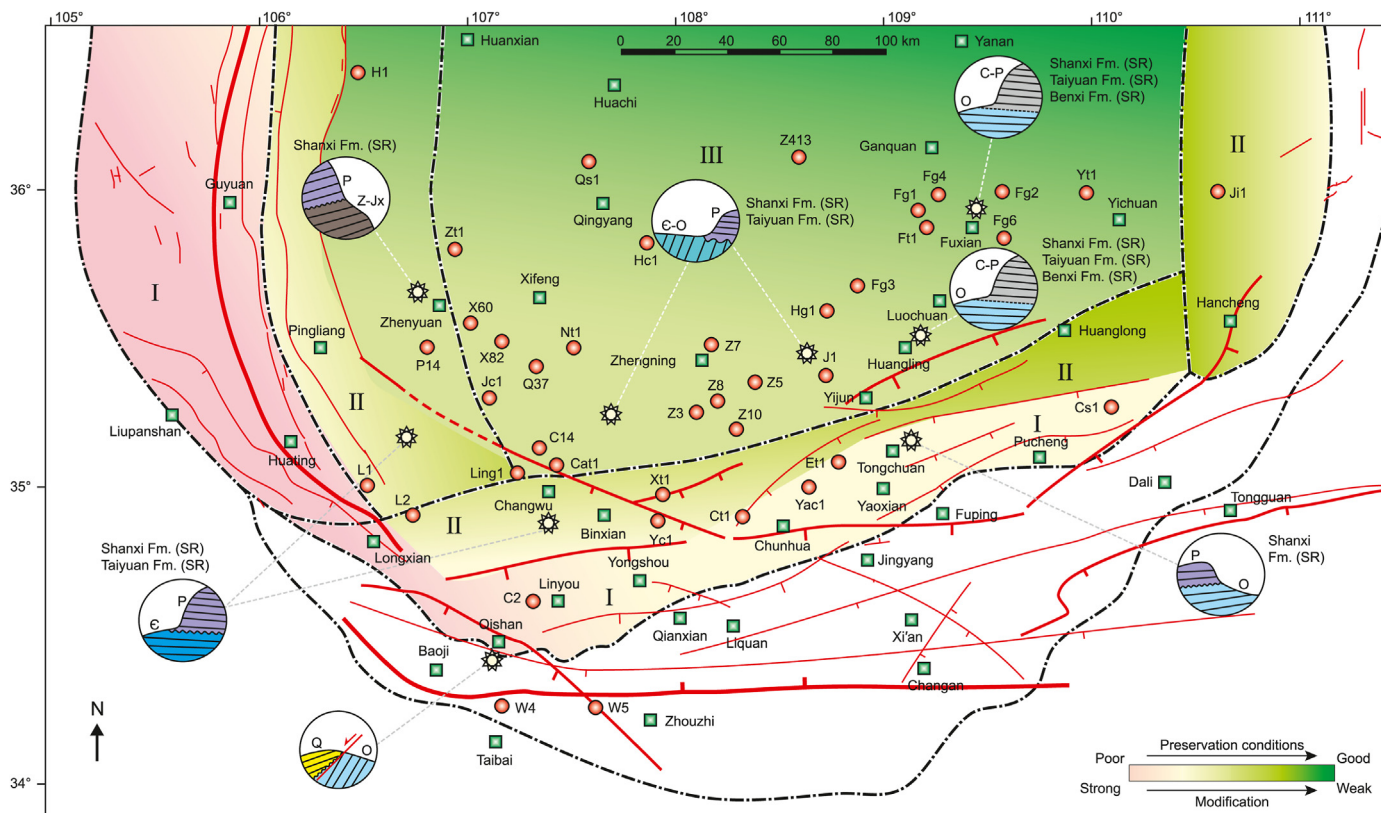


Fig. 9. Comprehensive evaluation on the hydrocarbon preservation conditions under the constraints of the fault distribution characteristics and the spatial and temporal evolutionary characteristics during the later modification. Note: Fm.-Formation, SR-Source rock, I-poor preservation (strong modification), II-moderate preservation (moderate modification), III-good preservation (weak modification).

poor oil and gas preservation conditions. In some areas, such as to the west of the Shajingzi and Binxian faults in the Tianhuan Depression, to the north of the Tianjiazui and Laolongshan faults in the Weibei Uplift and within the Jinshaan Tectonic Zone in the eastern part of the southern Ordos Basin, Cambrian-Ordovician strata are in unconformable contact with the Permian Shanxi Formation and have good oil and gas preservation conditions. The Shaanbei Slope and other areas to the east of the Shajingzi and Binxian faults in the Tianhuan Depression were characterized by weaker deformation, later uplift and less denudation. The Cambrian-Ordovician strata are separated from Carboniferous-Permian strata (i.e., the Benxi, Taiyuan and Shanxi formations) by an angular unconformity. These areas and strata have relatively good oil and gas preservation conditions (Fig. 9).

The fission-track results revealed that the southern part of the basin was characterized by early uplift in the south and later uplift in the north since the Yanshanian Orogeny. The southwestern area experienced the earliest uplift. During the Himalayan Orogeny, growth of the Tibetan Plateau and formation of the Liupanshan thrust zone, Qinling orogenic belt and peripheral graben resulted in accelerated uplift (i.e., since 40 Ma) and fault reactivation in the southern Ordos Basin. This faulting activity may have resulted in the destruction of petroleum reservoirs and loss of oil and gas (Fig. 10). In summary, the tectono-thermal evolution of the southern Ordos Basin had an important role in controlling petroleum generation, accumulation and preservation. The main petroleum generation and accumulation stages were at the end-Late Cretaceous, which is consistent with the timing of thermal events, maximum burial and paleo-temperatures (Figs. 8 and 10). Later uplift, cooling and denudation controlled the oil and gas

preservation conditions (Figs. 6, 8–10). These observations can guide future oil and gas exploration in the Ordos Basin.

7. Conclusions

- (1) Present temperatures in the southern Ordos Basin are generally lower in the southeast and higher in the northwest and are controlled by the monocline-like stratigraphy and structure. Geothermal gradient ranges from 24 to 30 °C/km and heat flow varies between 58 and 69 mW/m², which is a medium-temperature basin.
- (2) Paleo-temperatures of the basin were higher than the present values and the thermal maturity of the source rocks was controlled by the highest paleo-temperatures. The R_o values of the Triassic strata are >0.7% and these rocks have reached medium-mature oil generation stage. The R_o values of the Permian-Ordovician strata are >1.8% and these rocks have reached the over-mature dry gas generation stage.
- (3) The southern Ordos Basin has experienced multiple tectonic events in the Late Ordovician (452 Ma), Late Triassic (215 Ma), Late Jurassic (165–160 Ma), End-Early Cretaceous (110–100 Ma) and Cenozoic (40 Ma). A large-scale tectono-thermal event occurred at 110–100 Ma, which controlled the highest paleo-temperatures, thermal maturity and peak period of petroleum generation and accumulation.
- (4) Multiple stages of tectonism resulted in the development of fault systems. Since the Late Cretaceous, the basin has experienced large-scale uplift and extensive transformation. This may have destroyed petroleum reservoirs and preservation and led to the loss of petroleum.

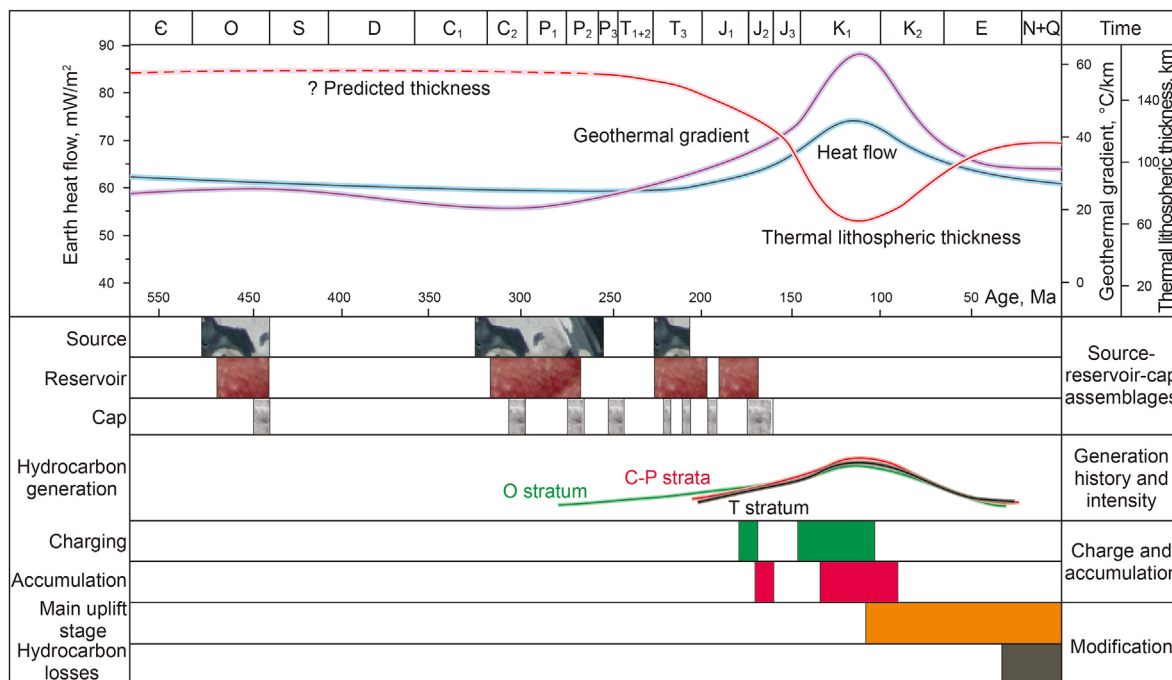


Fig. 10. Potential relationships between tectono-thermal evolution history and hydrocarbon generation, accumulation, later modification and preservation condition of the southern Ordos Basin.

(5) Large-scale petroleum generation and accumulation during the Early Cretaceous in the southern Ordos Basin were mainly controlled by deep processes involving lithospheric extension, thinning and destruction. The petroleum generation, accumulation and preservation in the southern Ordos Basin is one of the most important responses to these deep lithospheric processes.

Declaration of competing interest

The authors declare that they have no known competing financial interests or personal relationships that could have appeared to influence the work reported in this paper.

Acknowledgments

We thank three anonymous reviewers for their critical and constructive comments that improved the manuscript. We also thank the PetroChina Changqing Oilfield Company and SINOPEC Wuxi Research Institute of Petroleum Geology for their supports to this study. This work was supported by the National Natural Science Foundation of China (Grant Nos. 42102164, 42241204, 41630312 and 42272174) and the PetroChina Changqing Oilfield Company Science and Technology Major Project (ZDZX 2021-01).

Appendix A. Supplementary data

Supplementary data to this article can be found online at <https://doi.org/10.1016/j.petsci.2023.12.006>.

References

Barker, C.E., Pawlewicz, M.J., 1986. The correlation of vitrinite reflectance with maximum temperature in humic organic matter. In: Buntebarth, G., Stegena, L. (Eds.), *Paleogeothermics Lecture Notes in Earth Sciences*, vol. 5. Springer, Berlin, Heidelberg, pp. 79–93. <https://doi.org/10.1007/BFb0012103>.
 Cao, Y.C., Yuan, G.H., Yang, H.J., et al., 2022. Current situation of oil and gas

exploration and research progress of the origin of high-quality reservoirs in deep-ultra-deep clastic reservoirs of petroliferous basins. *Acta Petrol. Sin.* 43 (1), 112–140. <http://www.syx-b-cps.com.cn/CN/10.7623/syxb202201010> (In Chinese with English abstract).
 Chen, Q.H., Li, W.H., Guo, Y.Q., Liang, J.W., Cui, J.P., 2006. Turbidite systems and the significance of petroleum exploration of Yanchang Formation in the southern Ordos Basin. *Acta Geol. Sin.* 80 (5), 656–663. [https://doi.org/10.1016/S1005-8885\(07\)60042-9](https://doi.org/10.1016/S1005-8885(07)60042-9) (In Chinese with English abstract).
 Chen, Q.H., Li, W.H., Gao, Y.X., Guo, Y.Q., Feng, J.P., Zhang, D.F., Cao, H.X., Liang, J.W., 2007. The deep-lake deposit in the upper triassic Yanchang Formation in Ordos Basin, China and its significance for oil-gas accumulation. *Sci. China Earth Sci.* 50 (Suppl. 2), 47–58. <https://doi.org/10.1007/s11430-007-6029-7>.
 Chen, Y., Li, J., Miao, P., Chen, L.L., Zhao, H.L., Wang, C., Yang, J., 2022. Relationship between the tectono-thermal events and sandstone-type uranium mineralization in the southwestern Ordos Basin, Northern China: insights from apatite and zircon fission track analyses. *Ore Geol. Rev.* 143, 104792. <https://doi.org/10.1016/j.oregeorev.2022.104792>.
 Dai, J.X., Ni, Y.Y., Qin, S.F., Huang, S.P., Peng, W.L., Han, W.X., 2018. Geochemical characteristics of ultra-deep natural gas in the Sichuan Basin, SW China. *Petrol. Explor. Dev.* 45 (4), 619–628. [https://doi.org/10.1016/S1876-3804\(18\)30067-3](https://doi.org/10.1016/S1876-3804(18)30067-3).
 Dong, Y.P., Yang, Z., Liu, X.M., Sun, S.S., Li, W., Cheng, B., Zhang, F.F., Zhang, X.N., He, D.F., Zhang, G.W., 2016. Mesozoic intracontinental orogeny in the qinling Mountains, central China. *Gondwana Res.* 30, 144–158. <https://doi.org/10.1016/j.jgr.2015.05.004>.
 Du, J.H., Li, X.B., Bao, H.P., Xu, W.L., Wang, Y.T., Huang, J.P., Wang, H.B., Wangyan, R., Wang, J., 2019. Geological conditions of natural gas accumulation and new exploration areas in the Mesoproterozoic to Lower Paleozoic of Ordos Basin, NW China. *Petrol. Explor. Dev.* 46 (5), 820–835. [https://doi.org/10.1016/S1876-3804\(19\)60246-6](https://doi.org/10.1016/S1876-3804(19)60246-6).
 Fang, Z.K., 1986. Variation characteristics of total organic carbon content during the thermal evolution of organic mudstone. *J. Northwest. Polytech. Univ.* 3 (3), 18–20 (In Chinese with English abstract).
 Fu, J.H., Fan, L.Y., Liu, X.S., Hu, X.Y., Li, J.H., Ji, H.K., 2019. New progresses, prospects and countermeasures of natural gas exploration in the Ordos Basin. *China Petrol. Explor.* 24 (4), 418–430. <http://www.cped.cn/CN/10.3969/j.issn.1672-7703.2019.04.002> (In Chinese with English abstract).
 Gleadow, A.J.W., Duddy, I.R., Green, P.F., Lovering, J.F., 1986. Confined fission track lengths in apatite: a diagnostic tool for thermal history analysis. *Contrib. Mineral. Petrol.* 94, 405–415. <https://doi.org/10.1007/BF00376334>.
 He, Z.X., 2003. *Evolution and Petroleum Characteristics of Ordos Basin*. Petroleum Industry Press, Beijing, pp. 5–21 (In Chinese).
 Jacobo, H., 1989. Classification, structure, genesis and practical importance of natural solid oil bitumen (“migrabitumen”). *Int. J. Coal Geol.* 11 (1), 65–79. [https://doi.org/10.1016/0166-5162\(89\)90113-4](https://doi.org/10.1016/0166-5162(89)90113-4).
 Jia, C.Z., Pang, X.Q., 2015. Research processes and main development directions of deep hydrocarbon geological theories. *Acta Petrol. Sin.* 36 (12), 1457–1469. <http://www.syx-b-cps.com.cn/CN/10.7623/syxb201512001> (In Chinese with

- English abstract).
- Ketchum, R.A., 2005. Forward and inverse modeling of low-temperature thermochronometry data. *Rev. Mineral. Geochem.* 58, 275–314. <https://doi.org/10.2138/rmg.2005.58.11>.
- Lei, P.P., 2015. Tectonic evolution and its influence on the Ordovician oil and gas accumulation conditions in southwest Ordos Basin. Master's Dissertation. Northwest University (In Chinese).
- Li, W.H., Ren, Z.L., 2010. Study on Geological Conditions of Petroleum Accumulation in Southeast Ordos Basin. Research Report on Major Scientific Research Projects of Changqing Oilfield Company, PetroChina (In Chinese).
- Li, Y.N., Liu, W.H., Wang, X.F., Jing, X.H., Liu, P., Zhang, D.D., Luo, H.Y., Wang, Q.T., Pei, L.X., Zhai, G.H., 2021. Potential causes of depleted $\delta^{13}\text{C}$ carb excursions in Ordovician marine carbonates, Ordos Basin, China. *Mar. Petrol. Geol.* 134, 105331. <https://doi.org/10.1016/j.marpetgeo.2021.105331>.
- Liang, Y., Ren, Z.L., Wang, Y.L., Shi, Z., 2011a. Characteristics of fluid inclusions and reservoiring phases in the Yanchang Formation of Zichang area, the Ordos Basin. *Oil Gas Geol.* 32 (2), 182–191. <http://ogg.pepris.com/CN/10.11743/ogg20110204> (In Chinese with English abstract).
- Liang, Y., Ren, Z.L., Shi, Z., Zhao, X.Y., Yu, Q., Shi, Z., 2011b. Classification of hydrocarbon accumulation phases of the Yanchang Formation in the fuxian-zhengning area, Ordos Basin. *Acta Petrol. Sin.* 32 (5), 741–748. <http://www.syx-b-cps.com.cn/CN/10.7623/syxb201105002> (In Chinese with English abstract).
- Liu, J.Z., Chen, H.H., Li, J., Hu, G.Y., Shan, X.Q., 2005. Using fluids inclusion of reservoir to determine hydrocarbon charging orders and times in the Upper Paleozoic of Ordos Basin. *Geol. Sci. Technol. Inf.* 24 (4), 60–66. <https://doi.org/10.1360/gso50303> (In Chinese with English abstract).
- Liu, Q.Y., Jin, Z.J., Wang, Y., Han, P.L., Tao, Y., Wang, Q.C., Ren, Z.L., Li, W.H., 2012. Gas filling pattern in Paleozoic marine carbonate reservoir of Ordos Basin. *Acta Petrol. Sin.* 28 (3), 847–858. <https://doi.org/10.2110/palo.2011.p11-036r> (In Chinese with English abstract).
- Liu, R.C., Ren, Z.L., Yang, P., He, H.Y., Smith, T.M., Guo, W., Wu, L., 2021. Mesozoic tectono-thermal event of the Qinshui Basin, central north China craton: insights from illite crystallinity and vitrinite reflectance. *Front. Earth Sci.* 9, 765497. <https://doi.org/10.3389/feart.2021.765497>.
- Ma, Y.S., Cai, X.Y., Zhao, P.R., Zhang, X.F., 2010. Mechanism and the model of carbonates reservoir property evolution in deep-buried carbonate. *Acta Geol. Sin.* 84 (8), 1087–1094. <https://doi.org/10.19762/j.cnki.dizhixuebao.2010.08.001> (In Chinese with English abstract).
- Mao, J., Wang, Y., Zhang, Z., Yu, J., Niu, B.G., 2003. Geodynamic settings of Mesozoic large-scale mineralization in North China and adjacent areas. *Sci. China Earth Sci.* 46, 838–851. <https://doi.org/10.1007/BF02879527>.
- Pang, X.Q., Fang, Z.K., Chen, Z.M., 1988. Ancient abundance of organic matter and its calculation method. *Acta Petrol. Sin.* 9 (1), 17–24. <http://www.syx-b-cps.com.cn/CN/10.7623/syxb198801003> (In Chinese with English abstract).
- Peng, H., Wang, J.Q., Massimiliano, Z., Liu, C.Y., Han, P., Zhang, S.H., 2018. Late Triassic-Early Jurassic uplifting in eastern Qilian Mountain and its geological significance: evidence from apatite fission track thermochronology. *Earth Sci.* 43 (6), 1983–1996. <https://doi.org/10.3799/dqkx.2018.608> (In Chinese with English abstract).
- Petersen, H.L., Sherwood, N., Mathiesen, A., Fyhn, M.B.W., Dau, N.T., Russell, N., Bojesen-Koefoed, J.A., Nielsen, L.H., 2009. Application of integrated vitrinite reflectance and FMM analyses for thermal maturity assessment of the northeastern Malay Basin, offshore Vietnam: implications for petroleum prospectivity evaluation. *Mar. Petrol. Geol.* 26, 319–332. <https://doi.org/10.1016/j.marpetgeo.2008.04.004>.
- Qi, L.X., 2016. Oil and gas breakthrough in ultra-deep Ordovician carbonate formations in Shuntuoguole uplift, Tarim Basin. *China Petrol. Explore* 21 (3), 38–51. <http://www.cped.cn/CN/Y2016/V21/I3/38> (In Chinese with English abstract).
- Qiu, N.S., Chang, J., Zuo, Y.H., Wang, J.Y., Li, H.L., 2012. Thermal evolution and maturation of lower Paleozoic source rocks in the Tarim Basin, northwest China. *AAPG (Am. Assoc. Pet. Geol.) Bull.* 96, 789–821. <https://doi.org/10.1306/09071111029>.
- Ren, Z.L., 1995. Application of apatite fission track analysis method to the study of thermal history of the Ordos Basin. *Chin. J. Geophys.* 38 (2), 235–247 (In Chinese with English abstract).
- Ren, Z., Zhang, S., Gao, S., Cui, J., Xiao, Y.Y., Xiao, H., 2007. Tectonic thermal history and its significance on the formation of oil and gas accumulation and mineral deposit in Ordos Basin. *Sci. China Earth Sci.* 50, 27–38. <https://doi.org/10.1007/s11430-007-6022-1>.
- Ren, Z.L., Liang, Y., 2010. Research on Resource Potential of Zichang Oil Production Plant. Research Project Report of Yanchang Oilfield Co., Ltd. (In Chinese).
- Ren, Z.L., Cui, J.P., Li, J.B., Wang, J., Guo, K., Wang, W., Tian, T., Li, H., Cao, Z.P., Yang, P., 2014a. Tectonic-thermal history reconstruction of ordovician in the Weiwei uplift of Ordos Basin. *Acta Geol. Sin.* 88 (11), 2044–2056 (In Chinese with English abstract).
- Ren, Z.L., Li, W.H., Liang, Y., Wu, X.Q., Yu, Q., Ren, L., Wang, W., 2014b. Tight oil reservoir formation conditions and main controlling factors of Yanchang Formation in southeastern Ordos Basin. *Oil Gas Geol.* 35 (2), 190–198. <http://ogg.pepris.com/CN/Y2014/V35/I2/190> (In Chinese with English abstract).
- Ren, Z.L., Tian, T., Li, J.B., Wang, J.P., Cui, J.P., Li, H., Tang, J.Y., Guo, K., 2014c. Review on methods of thermal evolution history in sedimentary basins and thermal evolution history reconstruction of superimposed basins. *J. Earth Sci. Environ.* 36, 1–20. <https://doi.org/10.3969/j.issn.1672-6561.2014.03.003> (In Chinese with English abstract).
- Ren, Z.L., Cui, J.P., Guo, K., Tian, T., Li, H., Wang, W., Yang, P., Cao, Z.P., 2015. Fission-track analysis of uplift times and processes of the Weiwei uplift in the Ordos Basin. *Chin. Sci. Bull.* 60, 1298–1309. <https://doi.org/10.1360/N972014-00617> (In Chinese with English abstract).
- Ren, Z.L., Yu, Q., Cui, J.P., Qi, K., Chen, Z.J., Cao, Z.P., Yang, P., 2017. Thermal history and its controls on oil and gas of the Ordos Basin. *Earth Sci. Front.* 24 (3), 137–148. <https://www.earthsciencefrontiers.net.cn/CN/10.13745/j.esf.2017.03.012> (In Chinese with English abstract).
- Ren, Z.L., Qi, K., Yang, G.L., Cui, J.P., Yang, P., Wang, K., 2020a. Research status and existing problems of relationship between deep thermal evolution history and oil and gas in sedimentary basins, 1–7 *Unconv. Oil Gas* 7 (3), 15 (In Chinese with English abstract).
- Ren, Z.L., Qi, K., Liu, R.C., Cui, J.P., Chen, Z.P., Zhang, Y.Y., Yang, G.L., Ma, Q., 2020b. Dynamic background of Early Cretaceous tectonic thermal events and its control on various mineral accumulations such as oil and gas in the Ordos Basin. *Acta Petrol. Sin.* 36 (4), 1213–1234. <https://doi.org/10.18654/1000-0569/2020.04.15> (In Chinese with English abstract).
- Ren, Z.L., Cui, J.P., Qi, K., Yang, G.L., Chen, Z.J., Yang, P., Wang, K., 2020c. Control effects of temperature and thermal evolution history of deep and ultra-deep layers on hydrocarbon phase state and hydrocarbon generation history. *Nat. Gas Ind-B* 7, 453–461. <https://doi.org/10.1016/j.ngib.2020.09.003>.
- Ren, Z.L., Qi, K., Li, J.B., Huo, X.J., Cui, J.P., Yang, P., Wang, K., Chen, Z.J., Yang, G.L., 2021. Thermodynamic evolution and hydrocarbon accumulation in the Ordos Basin. *Oil Gas Geol.* 42 (5), 1030–1042. <http://ogg.pepris.com/CN/10.11743/ogg20210502> (In Chinese with English abstract).
- Shi, Z.L., Liu, F.S., 1999. Metallogenic systems about mesozoic metalliferous deposits in north taihang Shan-yan Shan area. *Earth Sci. Front.* 6 (2), 297–304. <https://www.earthsciencefrontiers.net.cn/CN/Y1999/V6/I2/0> (In Chinese with English abstract).
- Song, L.J., Mu, Q.H., Li, A.R., Li, L., 2013. Fission-track thermal evolution history in the formation age of Yaoshan Formation. *Coal Geol. Explor.* 41 (4), 1–4. <https://doi.org/10.3969/j.issn.1001-1986.2013.04.001> (In Chinese with English abstract).
- Sun, L.D., Zou, C.N., Zhu, R.K., Zhang, Y., Zhang, S.C., Zhang, B.M., Zhu, G.Y., Gao, Z.Y., 2013. Formation, distribution and potential of deep hydrocarbon resources in China. *Petrol. Explor. Dev.* 40 (6), 687–695. [https://doi.org/10.1016/S1876-3804\(13\)60093-2](https://doi.org/10.1016/S1876-3804(13)60093-2).
- Sun, S.H., Liu, S.S., 1996. Tectono-thermal events in Ordos Basin, China. *Chin. Sci. Bull.* 41 (24), 2070–2073. <https://doi.org/10.1360/CSB1997-42-3-306>.
- Tian, T., Yang, P., Ren, Z.L., Fu, D.L., Zhou, S.X., Yang, F., Li, J., 2020. Hydrocarbon migration and accumulation in the Lower Cambrian to Neoproterozoic reservoirs in the Micangshan tectonic zone, China: new evidence of fluid inclusions. *Energy Rep.* 6, 721–733. <https://doi.org/10.1016/j.egyry.2020.03.012>.
- Tissot, B.P., Welte, D.H., 1978. *Petroleum Formation and Occurrence*. Springer-Verlag, Berlin, pp. 1–554. <https://doi.org/10.1007/978-3-642-87813-8>.
- Wang, P.W., Chen, Z.H., Jin, Z.J., Guo, Y.C., Chen, X., Jiao, J., Guo, Y., 2019. Optimizing parameter “total organic carbon content” for shale oil and gas resource assessment: taking west Canada sedimentary basin Devonian Duvernay shale as an example. *Earth Sci.* 44 (2), 504–512. <https://doi.org/10.3799/dqkx.2018.191> (In Chinese with English abstract).
- Wang, D.Y., Lu, X.C., Zhang, X.J., Xu, S.J., Hu, W.X., Wang, L.S., 2007. Heat-model analysis of wall rocks below a diabase sill in Huimin Sag, China compared with thermal alteration of mudstone to carbargillite and hornfels and with increase of vitrinite reflectance. *Geophys. Res. Lett.* 34, L16312. <https://doi.org/10.1029/2007GL030314>.
- Wang, J.Q., Liu, C.Y., Zhao, H.G., Zhang, D.D., Massimiliano, Z., Peng, H., 2020. Uplift and exhumation events and thermochronological constraints at the end of Triassic in southwestern Ordos Basin. *Acta Petrol. Sin.* 36 (4), 1199–1212. <https://doi.org/10.18654/1000-0569/2020.04.14> (In Chinese with English abstract).
- Wang, X.X., Wang, T., Zhang, C.L., 2015. Granitoid magmatism in the Qinling orogen, central China and its bearing on orogenic evolution. *Sci. China Earth Sci.* 58, 1497–1512. <https://doi.org/10.1007/s11430-015-5150-2>.
- Wang, X.Z., Gao, S.L., Gao, C., 2014. Geological features of Mesozoic lacustrine shale gas in south of Ordos Basin, NW China. *Petrol. Explor. Dev.* 41 (3), 294–304. [https://doi.org/10.1016/S1876-3804\(14\)60037-9](https://doi.org/10.1016/S1876-3804(14)60037-9).
- Xiao, X.M., Song, Z.G., Liu, D.H., Liu, Z.F., Fu, J.M., 2000. The Tazhong hybrid petroleum system, Tarim Basin, China. *Mar. Petrol. Geol.* 17, 1–12. [https://doi.org/10.1016/S0264-8172\(99\)00050-1](https://doi.org/10.1016/S0264-8172(99)00050-1).
- Xiao, H., Li, J.X., Han, W., Yang, Q., 2013. The tectonic uplift time and evolution characteristics of Weiwei uplift in the south edge of Ordos Basin. *J. Xi'an Univ. Sci. Technol.* 33, 576–593 (In Chinese with English abstract).
- Xiong, X., Zhu, L.M., Zhang, G., Guo, A.L., Zheng, J., Jiang, H., 2019. Origin of the Xiaohokou skarn copper deposit and related granitoids in the Zha-Shan ore cluster area, South Qinling, China. *Ore Geol. Rev.* 114, 103–143. <https://doi.org/10.1016/j.oregeorev.2019.103143>.
- Xu, X.G., Chen, G., Liu, T., Kang, Y., Ren, S.F., Yan, F., 2017. Tectono-thermal evolution of Yanchang Formation in the jinsuoguan area of the southeastern Ordos Basin. *Geol. Sci. Technol. Inf.* 36 (3), 46–52 (In Chinese with English abstract).
- Yang, J.J., 2002. *Tectonic Evolution and Oil-Gas Distribution of Ordos Basin*. Petroleum Industry Press, Beijing (In Chinese).
- Yang, P., Ren, Z.L., Xia, B., Zhao, X.Y., Tian, T., Huang, Q.T., Yu, S.R., 2017. The Lower Cretaceous source rocks geochemical characteristics and thermal evolution history in the HaRi Sag, Yin-E Basin. *Petrol. Sci. Technol.* 35 (12), 1304–1313.

- <https://doi.org/10.1080/10916466.2017.1327969>.
- Yang, P., Ren, Z.L., Zhang, J.G., Xia, B., Tian, T., Cai, Z., Zhang, Y., 2018. Discussion of the coupling relationships between the cenozoic sedimentary-tectonic migration of the Weihe Basin and the uplift of the Weibei and east qinling areas. *Chinese J. Geol.* 53 (3), 876–892. <https://doi.org/10.12017/dzjx.2018.049> (In Chinese with English abstract).
- Yang, P., Wu, G.H., Ren, Z.L., Zhou, R., Zhao, J., Zhang, L., 2020. Tectono-thermal evolution of Cambrian–Ordovician source rocks and implications for hydrocarbon generation in the eastern Tarim Basin, NW China. *J. Asian Earth Sci.* 194, 104267. <https://doi.org/10.1016/j.jseae.2020.104267>.
- Yang, P., Ren, Z.L., Zhou, R.J., Cui, J., Qi, K., Fu, J., Li, J., Liu, X., Li, W., Wang, K., 2021a. Tectonic evolution and controls on natural gas generation and accumulation in the Ordovician system of the Ordos Basin, North China. *Energy Rep.* 7, 6887–6898. <https://doi.org/10.1016/j.egyr.2021.10.066>.
- Yang, P., Wu, G.H., Nuriel, P., Nguyen, A.D., Chen, Y., Yang, S., Feng, Y.-X., Ren, Z., Zhao, J.-X., 2021b. In situ LA-ICPMS U-Pb dating and geochemical characterization of fault-zone calcite in the central Tarim Basin, northwest China: implications for fluid circulation and fault reactivation. *Chem. Geol.* 568, 120125. <https://doi.org/10.1016/j.chemgeo.2021.120125>.
- Yang, P., Ren, Zhanli, Zhao, J.-x., Nguyen, A.D., Feng, Y.-x., Qi, K., Wang, K., 2021c. Tectonic evolution analysis constrained jointly by in-situ calcite U-Pb dating and apatite fission track for southwestern Ordos Basin. *Oil Gas Geol.* 42 (5), 1189–1201. <http://ogg.pepris.com/CN/10.11743/ogg20210516> (In Chinese with English abstract).
- Yang, S.Z., Jin, W.H., Li, Z.H., 2006. Multicycle superimposed basin form and evolution of the Ordos Basin. *Nat. Gas Geosci.* 17 (4), 494–498. <http://www.nggs.ac.cn/CN/10.11764/j.issn.1672-1926.2006.04.494> (In Chinese with English abstract).
- Yu, Q., Ren, Z.L., Zhu, Z.W., Tao, N., Wang, B.J., Li, C.C., 2018. Exhumation, cooling and erosion history of triassic oil shale since late cretaceous, binxian-tongchuan area of Ordos Basin. *Earth Sci.* 43 (6), 1839–1849. <https://doi.org/10.3799/dqkx.2018.596> (In Chinese with English abstract).
- Yu, Q., Ren, Z.L., Li, R.X., Tao, N., Qi, K., Jiang, C., Wang, B.J., 2019. Meso-Cenozoic tectonothermal history of Permian strata, Southwestern Weibei Uplift: insights from thermochronology and geothermometry. *Acta Geol. Sin.-Engl.* 93 (6), 1647–1661. <https://doi.org/10.1111/1755-6724.14367>.
- Yu, Q., Ren, Z.L., Li, R.X., Chung, L., Tao, N., Cui, J.P., Wang, B.J., Qi, K., Khaled, A., 2021. Cooling history of the southwestern Ordos Basin (northern China) since late jurassic: insights from thermochronology and geothermometry. *J. Asian Earth Sci.* 219, 104895. <https://doi.org/10.1016/j.jseae.2021.104895>.
- Yuan, W.G., Zhao, Y.M., 1996a. Characteristics and evolution of passive continental margin during Early Palaeozoic Era in southern Ordos. *J. Northwest For. Univ.* 26 (5), 451–454 (In Chinese with English abstract).
- Yuan, W.G., Wang, P., 1996b. On the caledonian movement in the southern eerdus basin. *J. Xi'an Coll. Geol.* 18 (1), 36–42 (In Chinese with English abstract).
- Zhang, C.L., Zhang, G.W., Yan, Y.X., Wang, Y., 2005. Origin and dynamic significance of Guangtoushan granitic plutons to the north of Mianlue zone in southern Qinling. *Acta Petrol. Sin.* 21 (3), 711–720. <https://doi.org/10.3321/j.issn:1000-0569.2005.03.012> (In Chinese with English abstract).
- Zhang, C.L., Wang, T., Wang, X.-X., 2008. Origin and tectonic setting of the Early Mesozoic granitoids in Qinling orogenic belt. *Geol. J. China Univ.* 14 (3), 304–316. <https://geology.nju.edu.cn/CN/Y2008/V14/I3/304> (In Chinese with English abstract).
- Zhang, Y.Q., Liao, C.Z., Shi, W., Hu, B., 2006. Neotectonic evolution of the peripheral zones of the Ordos Basin and geodynamic setting. *Geol. J. China Univ.* 12 (3), 285–297. <https://geology.nju.edu.cn/CN/Y2006/V12/I3/285> (In Chinese with English abstract).
- Zhang, Y.Q., Liao, C.Z., Shi, W., Zhang, T., Guo, F.F., 2007. On the jurassic deformation in and around the Ordos Basin. *Earth Sci. Front.* 14 (2), 182–196. <https://www.earthsciencefrontiers.net.cn/CN/Y2007/V14/I2/182> (In Chinese with English abstract).
- Zhai, M.G., 2011. Cratonization and the ancient North China Continent: a summary and review. *Sci. China Earth Sci.* 54 (8), 1110–1120. <https://doi.org/10.1007/s11430-011-4250-x>.
- Zhai, M.G., 2012. Evolution of the North China Craton and early plate tectonics. *Acta Geol. Sin.* 86 (9), 1335–1349 (In Chinese with English abstract).
- Zhao, G.C., Wang, Y.J., Huang, B.C., Dong, Y.P., Li, S.Z., Zhang, G.W., Yu, S., 2018. Geological reconstructions of the east asian blocks: from the breakup of Rodinia to the assembly of pangea. *Earth Sci. Rev.* 186, 262–286. <https://doi.org/10.1016/j.jearscrev.2018.10.003>.
- Zhao, W.Z., Hu, S.Y., Liu, W., Wang, T.S., Li, Y.X., 2014. Petroleum geological features and exploration prospect of deep marine carbonate rocks in China onshore: a further discussion. *Nat. Gas Ind-B* 1 (1), 14–23. <https://doi.org/10.1016/j.ngib.2014.10.002>.
- Zhu, J.H., Lv, J.H., Miu, J.J., Yuan, D.S., Zhang, Y.X., 2011a. Hydrocarbon generation potential of lower Paleozoic source rocks in southwestern margin of Ordos Basin. *Petrol. Geol. Exp.* 22 (6), 662–670. <https://doi.org/10.11781/sysydz201106662> (In Chinese with English abstract).
- Zhu, L.M., Zhang, G.W., Li, B., Guo, B., 2008. Main geological events, genetic types of metallic deposits and their geodynamical setting in the Qinling orogenic belt. *Bull. China Soc. Mineral Petrol. Geochem.* 27 (4), 384–390 (In Chinese with English abstract).
- Zhu, L.M., Zhang, G.W., Li, B., Guo, B., Yao, A.P., Gong, H.J., 2009. Some key metallogenic events of Qinling orogenic belt and their deposit examples. *J. Northwest For. Univ.* 39 (3), 381–391 (In Chinese with English abstract).
- Zhu, R.X., Chen, L., Wu, F.Y., Liu, J.L., 2011b. Timing, scale and mechanism of the destruction of the North China Craton. *Sci. China Earth Sci.* 54, 789–797. <https://doi.org/10.1007/s11430-011-4203-4>.
- Zhou, D.W., Zhao, Z.Y., Li, Y.d., et al., 1994. Geological Characteristics of Southwest Ordos Basin and its Relation to Qinling Orogenic Belt. Geological Press, Beijing (In Chinese).
- Zuo, Y.H., Qiu, N.S., Zhang, Y., Li, C.C., Li, J.P., Guo, Y.H., Pang, X.Q., 2011. Geothermal regime and hydrocarbon kitchen evolution of the offshore Bohai Bay Basin, North China. *AAPG (Am. Assoc. Pet. Geol.) Bull.* 95, 749–769. <https://doi.org/10.1306/09271010079>.
- Zuo, Y.H., Qiu, N.S., Hao, Q.Q., Pang, X.Q., Gao, X., Wang, X.-J., Luo, X.P., Zhao, Z.Y., 2015. Geothermal regime and source rock thermal evolution in the Chagan sag, Inner Mongolia, northern China. *Mar. Petrol. Geol.* 59, 245–267. <https://doi.org/10.1016/j.marpetgeo.2014.09.001>.